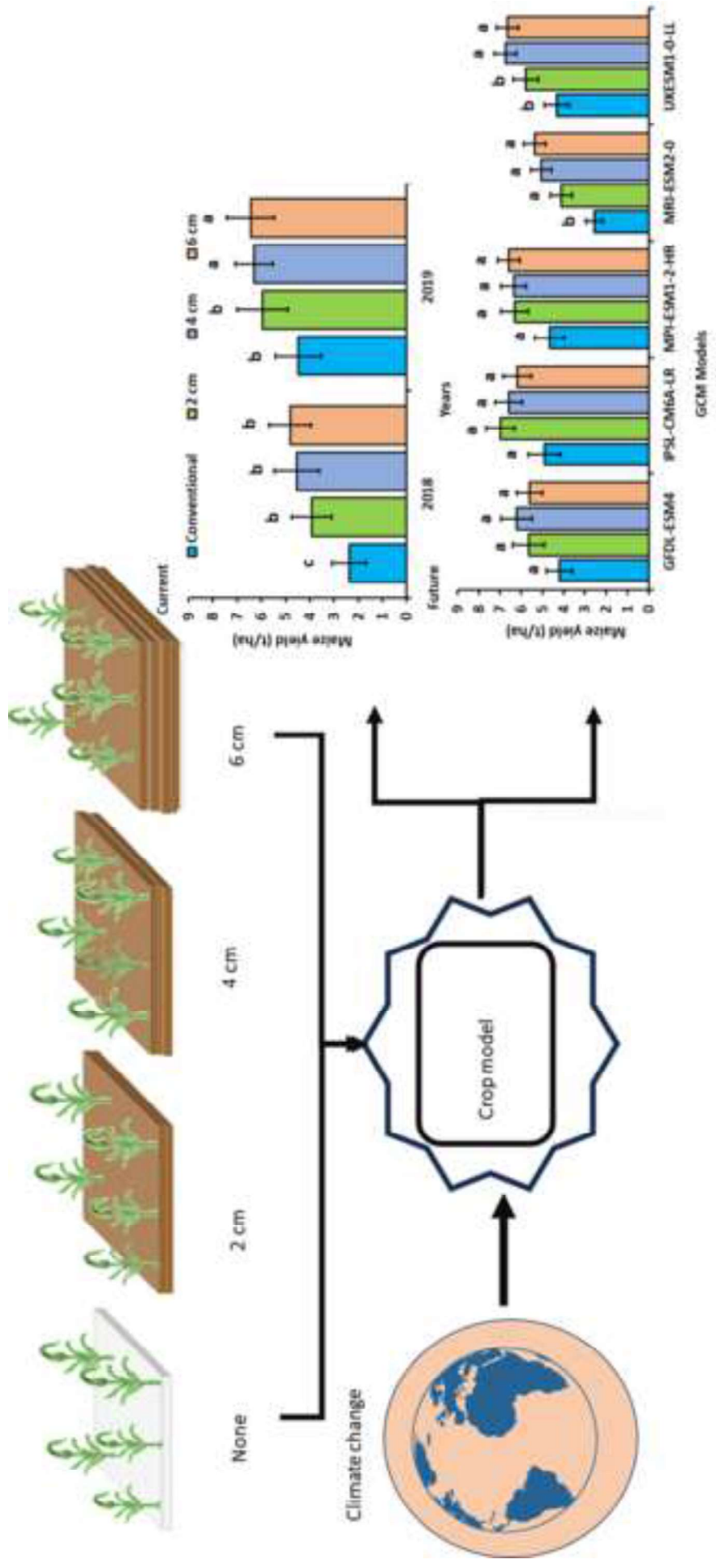


## Highlights

- Mulch and crop models guide adaptation in rainfed maize under climate change risks
- Mulching can improve maize yield now, but future impacts are less understood
- AquaCrop model accurately predicted yield, with  $R^2$  values of 0.84 - 0.95
- Mulching boosts yield by up to 40% under current conditions with 4 - 6 cm thickness
- Future yields may increase by 53% with 2 cm mulch under the SSP3-7.0 scenario



**Declaration of interests**

The authors declare that they have no known competing financial interests or personal relationships that could have appeared to influence the work reported in this paper.

The authors declare the following financial interests/personal relationships which may be considered as potential competing interests:

# 1 Straw Mulching Enhances Rainfed Maize Yield Under Climate Change Scenarios

2  
3 Alex Zizinga<sup>a d\*</sup>, Abel Chemura<sup>b</sup>, Alex C. Ruane<sup>c</sup>, Britta Tietjen<sup>a</sup>

4  
5 <sup>a</sup>Freie Universität Berlin, Institute of Biology, Theoretical Ecology, Königin-Luise-Str. 2/4, Gartenhaus, D-14195 Berlin,  
6 Germany

7 <sup>b</sup>University of Twente, Enschede, The Netherlands

8 <sup>c</sup>NASA Goddard Institute for Space Studies (GISS), New York, NY, United States of America

9 <sup>d</sup>Makerere University, P.O. Box 7062 Kampala, Uganda.

10 Corresponding author. E-mail address: [azizinga@gmail.com](mailto:azizinga@gmail.com)

## 11 Abstract

12 Maize cropping systems dominate crop land use in Sub-Saharan Africa (SSA), where rainfed agriculture  
13 is highly vulnerable to climate variability, exacerbating hunger and poverty. Effective soil water  
14 management practices (SWMPs), such as straw mulching, are known to improve water availability and  
15 enhance maize productivity. However, limited research studies have focused on straw mulch  
16 thicknesses and depth impact on maize rainfed production systems of SSA. This study evaluates the  
17 effects of different straw mulch thicknesses (2 cm, 4 cm, and 6 cm) on maize yield simulated using the  
18 AquaCrop model under the low (SSP1-2.6) and the high (SSP3-7.0) emission climate change scenarios  
19 from the IPCC's selected CMIP6 climate models. Field experiments with varying straw mulch  
20 thicknesses (2 cm, 4 cm, and 6 cm) were used to calibrate the AquaCrop model, which was then applied  
21 to simulate maize yields across current (2018 – 2019) and future (2020 – 2099) periods. Results showed  
22 that, straw mulch thickness significantly influences maize yields, with 4 cm and 6 cm treatments  
23 increasing maize yield by up to 40%. The 2 cm mulch, under the high emission scenario, led to a 53%  
24 yield increase, with the 4 cm mulch being identified as the optimal thickness for maximizing yield and  
25 water use efficiency (WUE). These findings suggest that straw mulch thickness should be adjusted to  
26 regional climatic conditions for optimal effectiveness. This study highlights the importance of  
27 integrating SWMPs with climate adaptation strategies to sustain maize productivity and improve food  
28 security in the context of climate change.

29 **Keywords:** AquaCrop model, soil water management, mulch thickness, maize yield, climate change.

30

31

32

33

34

35

36

37

38

39

40

41

42

43

44

45

46

47

48

49

50

51

52

53

54

55

56

57

58

59

60

61

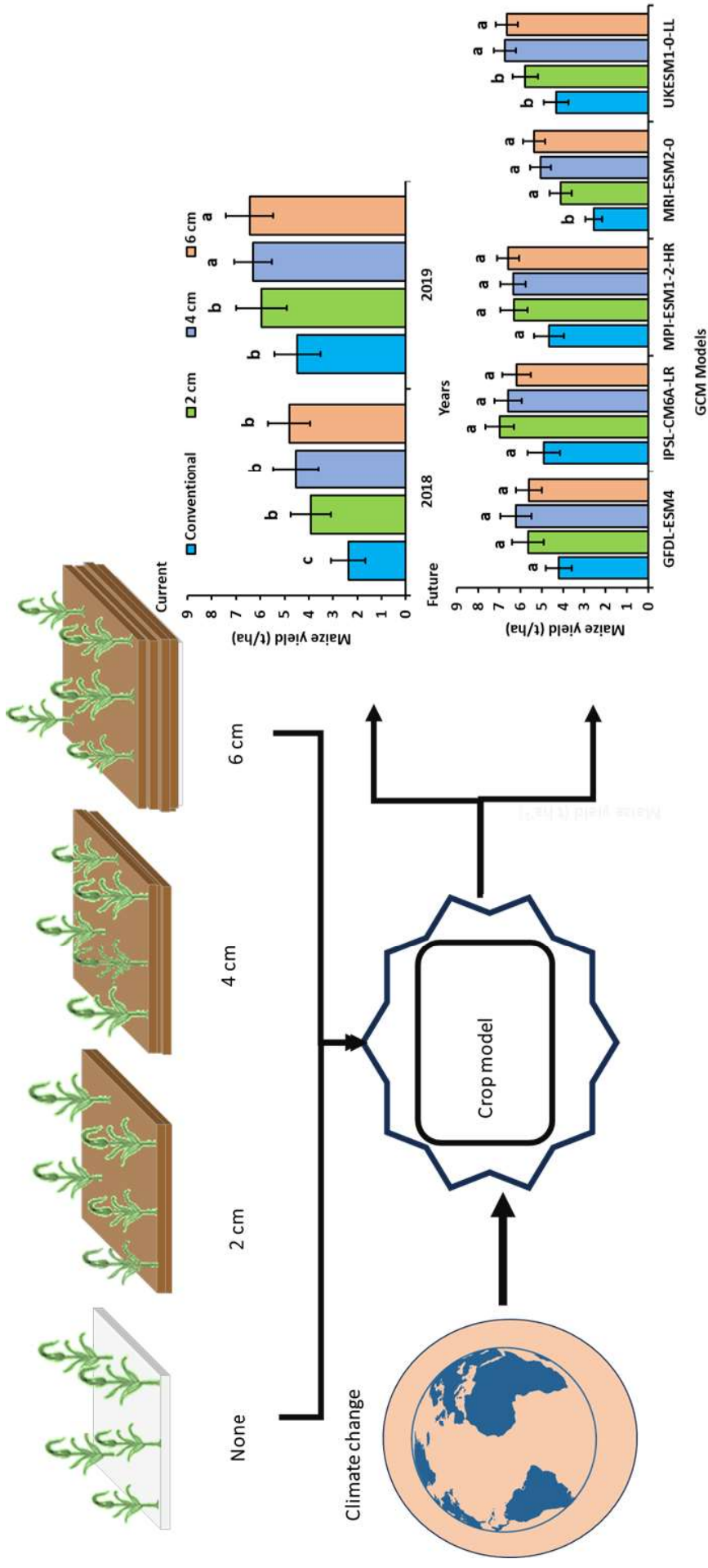
62

63

64

65

34 Graphical abstract



## 38 **1. Introduction**

39 Climate change is a pressing grand global challenge of the 21st century, affecting the livelihoods and  
40 natural resources of the Earth. It poses substantial implications for agriculture in sub-humid tropical  
41 regions dominated with rainfed production systems due to increasing water shortages and availability  
42 (Ayanlade et al., 2022; Dickerson et al., 2021). In Uganda, a country heavily dependent on rainfed  
43 agriculture, climate projections indicate heightened rainfall variability and rising temperatures that  
44 directly threaten soil moisture availability and crop productivity (Ayanlade et al., 2018; Harrison et al.,  
45 2019; Ongoma et al., 2018; Trambauer et al., 2013). This is a particular concern for high water-use  
46 crops like maize, which is widely cultivated and often intercropped to maximize land use efficiency  
47 (FOASTAT, 2017). Although maize accounts for nearly 30% of cereal production in Africa (Boote et  
48 al., 2015; Shiferaw et al., 2014) and plays a critical role in Uganda's food systems (Kaizzi et al., 2012),  
49 yields remain below global averages ( $< 2$  t/ha), largely due to inadequate adaptation to climatic stresses  
50 and limited soil water management practices to support optimal growth and productivity. Continuous  
51 cultivation without sufficient soil conservation measures has further exacerbated productivity losses  
52 affecting ~90% of smallholders (Okoboi, 2010; Kaizzi et al., 2012). Many practices such as half moon  
53 pits, contour bunds, Zai pits, cover crops, application of organic amendments such as compost and  
54 manure, tied ridges or contour bunds for water retention, among others have been reported in various  
55 regions across the sub-humid tropics of Africa (Biazin et al., 2012; Sawadogo et al., 2011).

56 Among the recommended climate change adaptation strategies, straw mulching has been recognized  
57 for its potential to improve soil moisture retention and reduce evapotranspiration under rainfed  
58 conditions (Kader et al., 2017; J. Y. Wang et al., 2021; X. Wang et al., 2014). However, the performance  
59 of different straw mulch thicknesses under current and future climate conditions remains poorly  
60 understood, especially in sub-humid zones characterized by high seasonal rainfall variability. While  
61 existing studies have explored soil water conservation technologies through modeling (Araya et al.,  
62 2015; Arumugam et al., 2023; Boote et al., 2015; Jägermeyr et al., 2021; Kikoyo and Nobert, 2016;  
63 Teshome et al., 2024; Zizinga et al., 2024), few have explicitly examined the long-term effects of straw  
64 mulch thicknesses on maize yields using climate projections based on the Coupled Model  
65 Intercomparison Project Phase 6 (CMIP6) scenarios. This limits evidence-based guidance on optimal  
66 mulch application for smallholder farmers facing increasing climate risks.

67 To address this knowledge gap, we used the AquaCrop biophysical model to evaluate the effects of  
68 varying straw mulch thicknesses (2 cm, 4 cm, and 6 cm) on maize productivity under current and  
69 projected climate change scenarios in mid-western Uganda. This region typifies rainfed maize systems  
70 in East Africa, where straw mulch is readily available but its application is constrained by insufficient  
71 data and localized recommendations.

72 By calibrating the model with experimental maize yield data collected over two growing seasons, we  
73 quantified the potential of straw mulch as a cost-effective, climate-resilient soil water management  
74 strategy. This study also informs Uganda’s Climate Smart Agriculture strategy, National Adaptation  
75 Plans (NAPs), and Nationally Determined Contributions (NDCs), helping to strengthen extension  
76 services and guide farmer-level implementation. Additionally, this provides one of the first long-term,  
77 process-based assessments of mulch thickness effects on maize yields under climate change conditions  
78 in Uganda. It offers actionable insights for improving soil water productivity in rainfed systems and  
79 highlights the need for targeted, locally adaptable technologies to build climate resilience in smallholder  
80 agriculture. While previous studies such as Zhang et al. (2020) explored similar themes in China, our  
81 work uniquely integrates localized SWMPs, CMIP6 datasets, and AquaCrop simulations to assess  
82 future impacts on maize yield and water use efficiency under Uganda agro-ecological conditions.

## 83 **2. Methodology**

### 84 **2.1 Study area**

85 The study was conducted in mid-western Uganda which lies within the western part of the country  
86 (Fig.1). This region experiences a sub-humid climate (Uganda Meteorological Authority, 2019), with  
87 an average annual precipitation of 1300 mm. Over 80 % of the rainfall occurs during two distinct  
88 seasons of March, April, and May while the second rainy season runs from September, October, and  
89 November each calendar year. During the maize growing period, the precipitation ranged between 429  
90 mm – 529 mm representative of typical growing conditions and seasonal distribution in the study area.

91 This area is particularly susceptible to the impacts of climate change due to various factors such as  
92 erratic weather patterns, dependence on rain-fed agriculture, and limited economic and institutional  
93 capacity to cope with and adapt to climate-related issues, including extended periods of drought  
94 (Zizinga et al., 2022).

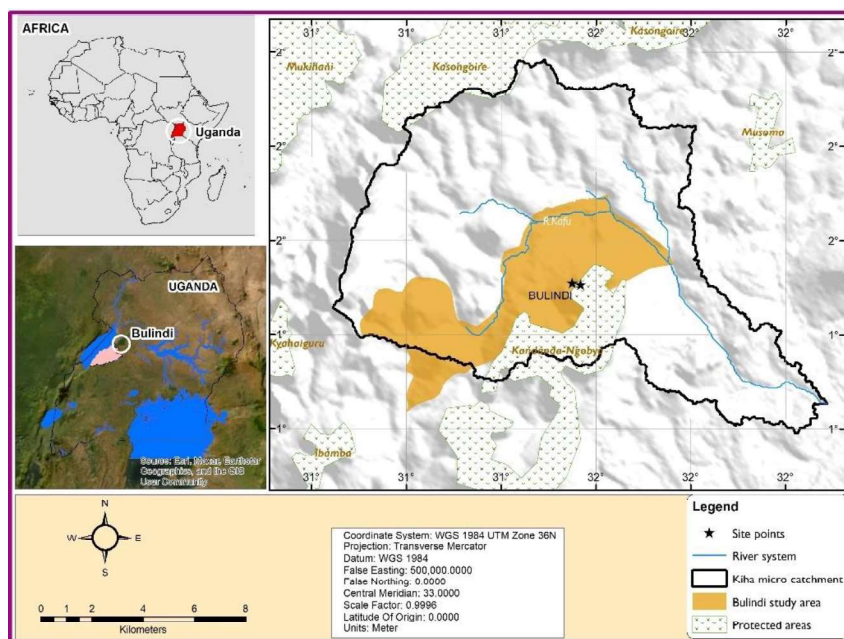


**Fig.1.** Map showing the location of the study area in Uganda and the insert shows the location of Uganda in Africa.

## 2.2. Field experiment

A completely randomized block design field experiment was conducted for two years (2018 – 2019). It was replicated four times in plots measuring 5 m × 5 m plots with border widths of 1 m and 2 m between plots, and blocks, respectively. Maize was planted at 5 cm depth at a spacing of 75 cm × 30 cm and thinning was done two weeks after planting to maintain one plant per hill, 111 plants in all the four selected soil water management practices of straw mulch of 2 cm (M2), 4 cm (M4), and 6 cm (M6) thicknesses covered at the soil surface in each treatment plot. Also, the conventional practice or control (C) consisted of land open tilling without any straw mulch. The plants were, 44,444 per hectare for all the four treatments. Seasonal maize biomass was collected by sub-sampling from each plot for the years 2018 – 2019 and the experiment focused on crop parameters for maize biomass in the above described SWMPs as treatments in the entire experiment.

The steps are shown in Fig.2 which have been followed to assess the impacts of selected soil water management practices (SWMPs) in Uganda. The first step was to calibrate the AquaCrop model using data of 2018, and validate with 2019 maize biomass from the observed field experiment.

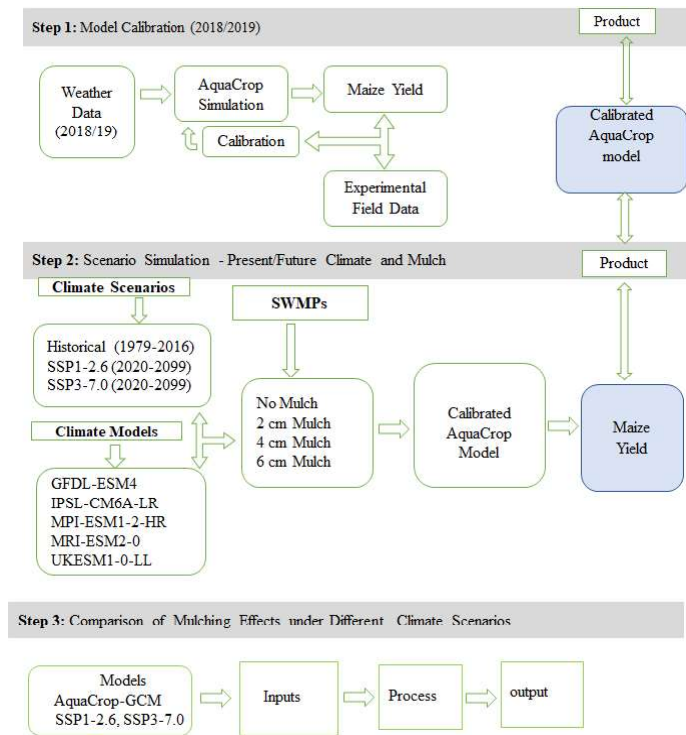


**Fig.2.** Methodology to assess the impacts of climate change and soil water management practices (SWMPs) on maize yields.

In the second step, the AquaCrop model was employed to project maize yields under various climate scenarios, including different SWMPs (Control, 2 cm, 4 cm, and 6 cm mulch thicknesses). The control or conventional treatment was without any SWMPs, and it is a typical farm cultivation practice used in the study area. Also, different time frames or periods are used in the study including the current climate period of 2018 – 2019 and three future periods of 2020 – 2039, 2040 – 2059, 2060 – 2079, 2080 – 2099), with two emission scenarios (SSP1-2.6 and SSP3-7.0). This step also involved a multidimensional comparison of the selected SWMPs under climate change conditions. All simulations were conducted at a spatial resolution of 0.5° x 0.5° (approximately 55 x 55 km<sup>2</sup>). The impacts of soil water management practices were assessed using integrated assessment models from the General Circulation Models (GCMs) of the sixth phase of the Coupled Model Intercomparison project (CMIP6). This combines and integrates climate change information from CMIP5-modeled RCPs and Shared Socioeconomic Pathways (SSPs) and Representative Concentration Pathways (Jia et al., 2022; Tebaldi et al., 2021). It also introduced new projection scenarios and our study included these in the CMIP6 model intercomparison project (O'Neill et al., 2016; Feng et al., 2025). The study focuses on scenarios SSP1-2.6 and SSP3-7.0 from the IPCC's 6th Assessment Report (IPCC, 2021), which represent a spectrum of potential future socioeconomic and emissions pathways (Arias et al., 2021). The SSP1-2.6 represents a moderate emission scenario requiring global cooperation and policy-driven efforts to mitigate climate change (Jia et al., 2022). It envisions a sustainable future with global warming likely

135 kept below 2°C, in line with the Paris Agreement goals. In contrast, SSP3-7.0 depicts a high greenhouse  
136 gas emissions scenario in future with substantial challenges for mitigation and adaptation due to  
137 minimal climate policy interventions (Arumugam et al., 2023). These scenarios integrate radiative  
138 forcing and socioeconomic influences, offering a diverse range of future conditions. Although these  
139 scenarios have received attention, there are limited studies in Uganda available on their long-term  
140 negative effects and potential solutions.

### 141 **2.3. Climate data, emissions scenarios, and climate indicators**

142 To evaluate the current climate and historical climate changes, this study utilizes the W5E5 dataset  
143 (Lange, 2019; Cucchi et al., 2020; Karger et al., 2023). This dataset integrates simulations from global  
144 weather models, satellite observations, and weather station data, covering the period from 1979 – 2016  
145 with daily temporal resolution and a global spatial resolution of 0.5° x 0.5° (approximately 55 km x 55  
146 km). The W5E5 dataset supports climate bias adjustment GCMs used in ISIMIP3b (Karger et al., 2023).  
147 This study incorporates future climate projections from ISIMIP3b, including bias-adjusted temperature  
148 (maximum and minimum), precipitation, and evapotranspiration (ET) simulations from five GCMs  
149 using downscaled CMIP6 data for detailed climate impact analysis.

150 The ISIMIP3b historical simulations span from 1850 – 2014, while future projections extend from 2015  
151 to 2100, all at a daily temporal resolution and a spatial resolution of 0.5° x 0.5°. The analysis uses the  
152 period from 1995 – 2014 as a reference and examines four future periods: 2020 – 2039, 2040 – 2059,  
153 2060 – 2079 and 2080 – 2099. The GCMs utilized in the ISIMIP3b project climate conditions with the  
154 GFDL-ESM4, IPSL-CM6A-LR, MPI-ESM1-2-HR, MRI-ESM2-0, and UKESM1-0-LL models  
155 (Lange, 2019). These models present varied projections due to inherent uncertainties in climate  
156 modeling which may originate from conservative estimates of potential climate changes anticipated  
157 with respective individual model results.

### 158 **2.4. AquaCrop model inputs**

159 In this study, we apply the AquaCrop, a widely used process-based crop model that simulates crop  
160 growth and yield as a function of soil-plant-atmosphere and water dynamics model (Doorenbos and  
161 Pruitt, 1977; Raes et al., 2006; Steduto et al., 2009). The crop input data in the model (Table 1) consisted  
162 of conservative parameters (maize crop phenology and water stress) and non-conservative parameters  
163 (plant density, time of sowing, germination period, rooting depth, growing degree days to reach  
164 flowering and maturity stages). AquaCrop model also uses daily weather data (air temperature, rainfall,  
165 reference evapotranspiration (ET<sub>o</sub>), and carbondioxide concentration), soil surface, and profile  
166 information with detailed crop management characteristics.

167 Crop yield is influenced by weather and other field inputs such as soil conditions and farmers'  
168 agronomic practices. Biophysical crop process-based simulation models like AquaCrop incorporate  
169 interactions among soil, water, plant, and atmospheric conditions. Additionally, the model calculates

170 crop productivity through processes such as canopy development, crop transpiration, biomass  
 171 accumulation, and final yield. It incorporates input variables related to climate, crop characteristics, soil  
 172 properties, and agricultural management practices (Raes et al., 2006), generating comprehensive  
 173 datasets covering crop growth, yield, and soil water dynamics.

174 Soil properties like soil texture, saturated hydraulic conductivity, bulk density, and other hydraulic  
 175 parameters were used as inputs for the AquaCrop model to create the soil file (Table 1). Bulk density  
 176 was determined using the undisturbed soil samples with the core method, and core samples were used  
 177 to measure saturated hydraulic conductivity ( $\theta_{ks}$ ) using the constant head method (Eijkelkamp Soil and  
 178 Water, 2017). The model's initial hydraulic parameters, including field capacity, permanent wilting  
 179 point, and soil water at saturation, were estimated using the Rosetta pedotransfer functions (Schaap et  
 180 al., 2001). In this study the capillary rise effects on soil water were not simulated due to the groundwater  
 181 table being below the rooting zone (Steduto et al., 2012), and other parameters were sourced from a  
 182 previous study (Zizinga et al., 2022).

183 **Table 1.** Soil hydraulic input parameters

| Depth (cm) | $\theta_s$ ( $\text{cm}^3 \text{cm}^{-3}$ ) | $\theta_{ks}$ ( $\text{cm d}^{-1}$ ) | $\theta_{fc}$ ( $\text{cm}^3 \text{cm}^{-3}$ ) | BD ( $\text{g cm}^{-3}$ ) | $\theta_{pw}$ ( $\text{cm}^3 \text{cm}^{-3}$ ) |
|------------|---|--------------------------------------|--|---------------------------|--|
| 0–10       | 0.45  | 10.6                                 | 0.33   | 1.38                      | 0.21   |
| 10–20      | 0.48  | 16.8                                 | 0.34   | 1.38                      | 0.21   |
| 20–30      | 0.48  | 9.3                                  | 0.36   | 1.36                      | 0.24   |
| 30–40      | 0.48  | 5.4                                  | 0.39   | 1.34                      | 0.26   |

184 **Note:**  $\theta_s$  is the saturated soil water content ( $\text{cm}^3 \text{cm}^{-3}$ );  $\theta_{ks}$  is the saturated hydraulic conductivity ( $\text{cm d}^{-1}$ );  $\theta_{fc}$  is  
 185 the field capacity ( $\text{cm}^3 \text{cm}^{-3}$ );  $\theta_{pw}$  is the permanent wilting point ( $\text{cm}^3 \text{cm}^{-3}$ ); **BD** is the bulk density ( $\text{g cm}^{-3}$ )  
 186 (Zizinga et al., 2022).

## 188 2.5. Model calibration

189 For this study, we used crop data from 2018 for calibration (Table 2) to simulate maize yields under  
 190 rainfed conditions in mid-western Uganda specifically for maize biomass yield while for validation, the  
 191 year of 2019 crop data was used by comparing the field measurements with simulated maize biomass  
 192 yield. The model best fit was statistically and graphically assessed with illustration using the R statistical  
 193 tool version 3.6.4 (R Core Team, 2020).

194 **Table 2.** Crop parameters of AquaCrop model

| Crop variables                     | Value, descriptions, and units |
|------------------------------------|--------------------------------|
| <b>Conservative Parameters</b>     |                                |
| Base temperature                   | 9 °C                           |
| Upper temperature                  | 34 °C                          |
| Maximum rooting depth              | 0.45 m                         |
| Canopy growth coefficient (CGC)    | 0.10988 per day CC increase    |
| Canopy decline coefficient (CDC)   | 0.1003 per day CC decrease     |
| <b>Non-Conservative Parameters</b> |                                |

|    |  |                                   |
|----|--|-----------------------------------|
| 1  | Effect of canopy cover in late season          | 60 CC effect on soil evaporation  |
| 2  | Soil surface covered by an individual seedling | 5 CC effect on soil evaporation   |
| 3  | Plant population per hectare                   | 44,444 ha <sup>-1</sup>           |
| 4  | Maximum canopy cover (CCx)                     | 0.84 (%) depends on plant spacing |
| 5  | Germination period                             | 5 -6 days                         |
| 6  | Time of sowing to maximum rooting depth        | 61 days                           |
| 7  | Senescence stage                               | 114 days                          |
| 8  | Maturity time                                  | 140 days                          |
| 9  | Time from sowing to flowering                  | 59 days                           |
| 10 | Flowering stage duration                       | 8 days                            |

11 195

12 196

13 197 **2.6. Soil Water Management (SWM) practices**

14 198 In this study, we implemented four soil water management practices with mulch at different thicknesses  
15 199 (2 cm, 4 cm, and 6 cm) in the AquaCrop model to assess yield impacts for current and future climate  
16 200 indicated in section 2.3.

17 201 First, mulching with straw dry grass is used to increase soil moisture storage in rainfed maize production  
18 202 and insulate the soil surface for soil evaporation (Kaer et al., 2018; El-Beltagi et al., 2019; Demo &  
19 203 Asefa, 2024). In the present study, mulch thicknesses of 2 cm, 4 cm, and 6 cm of straw mulch were  
20 204 used. Studies in southern Africa and the Loes Plateau of Northern China, have conducted studies on the  
21 205 adoption of mulch and its ability to increase water capture and storage, boosted maize yield, and  
22 206 enhance resilience to drought compared to conventional tillage practices (Biazin et al., 2012; Lin et al.,  
23 207 2016; Zhang et al., 2014; Zizinga et al 2022; Lamptey et al., 2020; Lipper et al., 2014; Mhlanga, 2021;  
24 208 Ngetich et al., 2014). Mulch as a soil and water conservation technique for crop production could  
25 209 increase maize yield and improve food security in tropical rainfed-based production systems.

26 210 **2.7 Simulation of mulch thicknesses in AquaCrop Model**

27 211 In the AquaCrop model, field management input parameters included the soil moisture collected using  
28 212 the Frequency Domain Reflectometry (FDR) probes (Delta-T Devices Ltd., 2006). Values of 85% for  
29 213 the control treatment and 86% for mulch of 2 cm, 4 cm, and 6 cm thicknesses were obtained from the  
30 214 field experimental plots and included as input in the AquaCrop model.

31 215 The application of AquaCrop model version 6.1 (<http://www.fao.org/aquacrop/en/>) considers  
32 216 alternatives of percentage soil cover like variations in mulch thicknesses (Steduto et al., 2009), and  
33 217 these model features were included in the present study for all the mulch thicknesses. The effect of  
34 218 mulch was simulated in the AquaCrop model with a percentage soil cover based on soil water content  
35 219 of 40%, 90%, and 100% for mulch of 2 cm (M2), 4 cm (M4), and 6 cm (M6) thickness, respectively,  
36 220 and this input was also applied in the calibration process based on recommended ranges for maize  
37 221 growing conditions (Hsiao et al., 2009).

38  
39  
40  
41  
42  
43  
44  
45  
46  
47  
48  
49  
50  
51  
52  
53  
54  
55  
56  
57  
58  
59  
60  
61  
62  
63  
64  
65

## 2.8. Statistical analysis

The model was evaluated using paired observed ( $O_i$ ) and simulated ( $P_i$ ) final maize biomass which were combined to determine the coefficient of determination ( $R^2$ ) describing the proportion of variance explained by the model with ranges between 0 and 1 as illustrated in (Eq 1), model efficiency (EF) an evaluation index for the EF that determines the relative change in residual variance between  $O_i$  and  $P_i$  with a range from 0 to 1 (Nash and Sutcliffe, 1970), and this is set in (Eq 2). Additional statistical measures including the root mean square error (RMSE t/ha) measuring the average magnitude of prediction errors computed to measure differences between  $O_i$  and  $P_i$  values as in (Eq 4) by Loague and Green, (1991), Willmott Index of agreement (d) depicting relative measure of error, ranging from 0 (disagreement) to 1 (agreement) in (Eq 3), and the percentage bias (PBIAS) computed to measure tendencies of larger and smaller  $O_i$  and  $P_i$  values with a range of 0% indicating a positive bias, while negative values specify under estimation due to model bias (Gupta et al., 1999), and this is shown in the (Eq 5).

$$R^2 = \frac{[\sum_{i=1}^n (O_i - \bar{O})(P_i - \bar{P})]^2}{\sum_{i=1}^n (O_i - \bar{O})^2 \times \sum_{i=1}^n (P_i - \bar{P})^2} \quad (\text{Eq 1}).$$

$$NSE = 1 - \frac{\sum_{i=1}^n (P_i - \bar{O})^2}{\sum_{i=1}^n (P_i - \bar{O})^2} \quad (\text{Eq 2})$$

$$d = 1 - \frac{\sum_{i=1}^n (|P_i - O_i|)^1}{\sum_{i=1}^n (|P_i| - O_i)^1} \quad (\text{Eq 3})$$

$$RMSE = \frac{\sqrt{\sum_{i=1}^n (O_i - P_i)^2}}{n} \quad (\text{Eq 4})$$

$$PBIAS = 100 \times \frac{\sqrt{\sum_{i=1}^n (O_i - P_i)}}{\sum_{i=1}^n O_i} \quad (\text{Eq 5})$$

Where  $O_i$  and  $P_i$  are the measured and simulated data,  $O_i$  and  $P_i$  are means for the both measured and simulated number of observations.

The  $n$  is the number of observations,  $P_i$  simulated observation and  $O_i$  measured observation.  $P_i| = P - M$  and  $O_i| = O_i - M$  ( $M$  is the mean of the observed variable). To analyze the scenarios, we used the AquaCrop model with data from various climate models (GCM-CMIP6) under different climate scenarios (SSP1-2.6 and SSP3-7.0) and applied three mulch thicknesses (2 cm, 4 cm, and 6 cm) with the control. The model was calibrated using historical observed data to ensure accuracy. We assessed the impact of each scenario on maize yield and water use efficiency (WUE) by comparing simulated results with observed data. Statistical metrics like RMSE and  $R^2$  were used to evaluate model

255 performance. The analysis identified the optimal mulch thickness and its effectiveness under different  
1 256 future climate conditions.

3 257

## 5 258 **3. Results**

### 7 259 **3.1. AquaCrop Calibration and Validation**

9 260 The model veracity was assessed by statistically comparing observed and simulated final maize biomass  
10 261 in response to soil water management practices (Fig.3). This compares predicted and measured biomass  
11 262 (t/ha) for: (a) C, (b) M2, (c) M4, and (d) M6, over the years 2018 and 2019. The coefficient of  
12 263 determination ( $R^2$ ) values for both years, indicate the goodness of fit. The higher  $R^2$  values signify better  
13 264 predictions.

14 265 For instance, C (a), M4 (c), and M6 (d) consistently show high  $R^2$  values for 2018 and 2019, reflecting  
15 266 their strong predictive accuracy. Conversely, M2 (b) has an  $R^2$  of 0.84 in 2018 and 0.95 in 2019,  
16 267 suggesting improvement in performance across years. The grey dotted lines depict the 95% confidence  
17 268 range for the regression lines, demonstrating the reliability of predictions (Fig.3).

18  
19  
20  
21  
22  
23  
24  
25  
26  
27  
28  
29  
30  
31  
32  
33  
34  
35  
36  
37  
38  
39  
40  
41  
42  
43  
44  
45  
46  
47  
48  
49  
50  
51  
52  
53  
54  
55  
56  
57  
58  
59  
60  
61  
62  
63  
64  
65

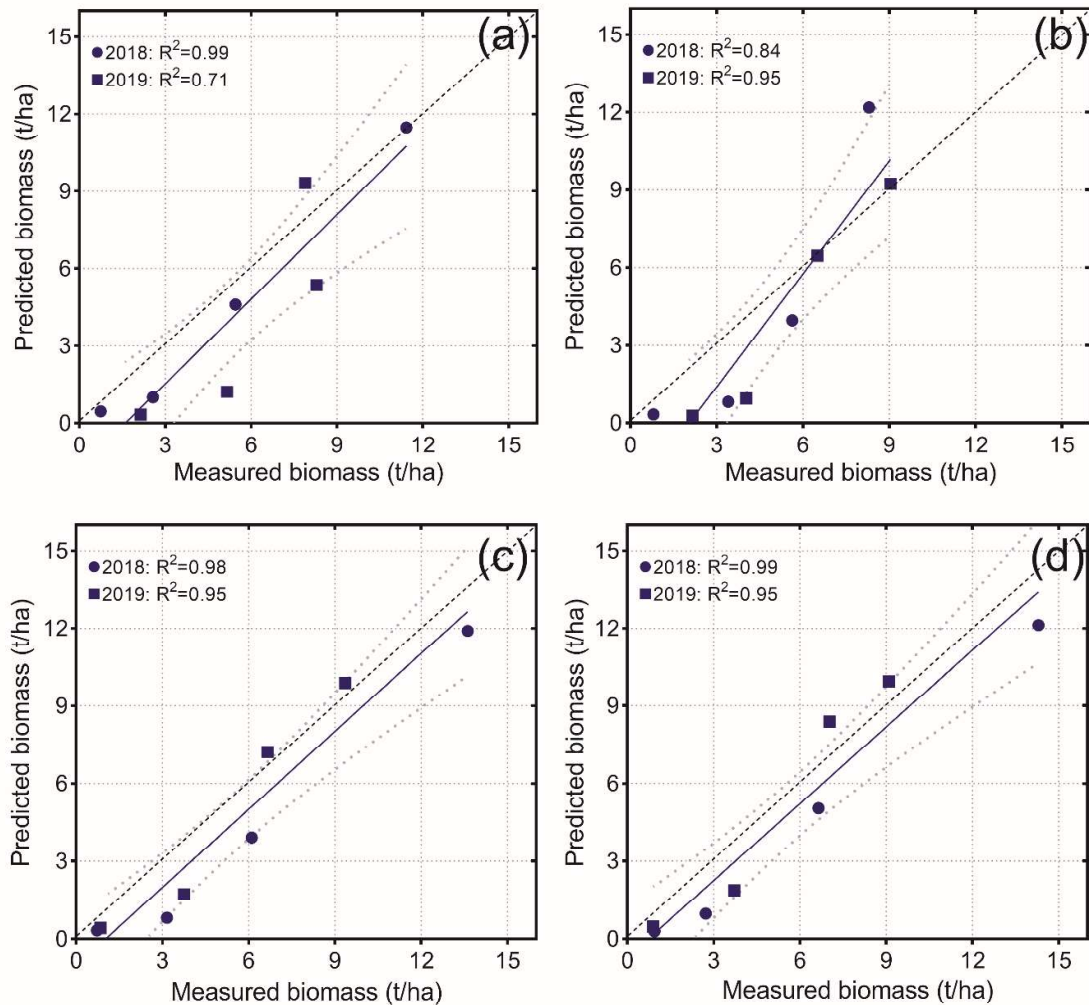


**Fig.3.** Comparison of observed and simulated maize total biomass: (a) C, (b) M2, (c) M4, and (d) M6.

Overall, the AquaCrop model performance can be observed by the EF values of 0.87 and 0.92 of grain yield (final biomass) under the observed and simulated values from the experimented soil water management practices (SWMPs) which correlated strongly to the final biomass accumulation (Table 3). The Root Mean Squared Error (RMSE) values also provide how well the AquaCrop model predictions matched the actual observed values as illustrated by the respective SWMPs (Table 3). The effect of mulch thickness is illustrated by the validated AquaCrop model and the model accuracy improves with increasing mulch thicknesses compared to the Control (2.56 t/ha), 2 cm (2.06 t/ha), 4 cm (1.38 t/ha), and 6 cm (1.16 t/ha). The 6 cm provides the best fit with even high biomass (14.30 t/ha), showing the smallest prediction error. Overall, higher mulch thickness treatments generally demonstrated better model performance, suggesting the efficiency of mulch to future maize yield increase.



**Table 4.** Changing in precipitation (mm year<sup>-1</sup>) for the four periods under SSP1-2.6 and SSP3-7.0 climate scenarios.

| GCM models           | Climate Scenarios |          |          |          | Change   |          |          | %Change |
|----------------------|-------------------|----------|----------|----------|----------|----------|----------|---------|
|                      | SSP1-2.6          | SSP3-7.0 | SSP1-2.6 | SSP3-7.0 | SSP1-2.6 | SSP3-7.0 | SSP1-2.6 |         |
| <b>GFDL-ESM4</b>     |                   |          |          |          |          |          |          |         |
| Baseline             | 1300.0            |          |          |          |          |          |          |         |
| 2020 - 2039          | 1051.4            | 1088.3   | -248.6   | -211.7   | -19.1    | -16.3    | -19.1    | -16.3   |
| 2040 - 2059          | 1105.7            | 1133.4   | -194.3   | -166.6   | -14.9    | -12.8    | -14.9    | -12.8   |
| 2060 - 2079          | 1117.2            | 1123.8   | -182.8   | -176.2   | -14.1    | -13.6    | -14.1    | -13.6   |
| 2080 - 2099          | 1090.6            | 1249.6   | -209.4   | -50.4    | -16.1    | -3.9     | -16.1    | -3.9    |
| <b>IPSL-CM6A-LR</b>  |                   |          |          |          |          |          |          |         |
| 2020 - 2039          | 1121.0            | 1137.0   | -179.0   | -163.0   | -13.8    | -12.5    | -13.8    | -12.5   |
| 2040 - 2059          | 1169.6            | 1116.7   | -130.4   | -183.3   | -10.0    | -14.1    | -10.0    | -14.1   |
| 2060 - 2079          | 1255.2            | 1218.9   | -44.8    | -81.1    | -3.4     | -6.2     | -3.4     | -6.2    |
| 2080 - 2099          | 1166.2            | 1410.2   | -133.8   | 110.2    | -10.3    | 8.5      | -10.3    | 8.5     |
| <b>MPI-ESM1-2-HR</b> |                   |          |          |          |          |          |          |         |
| 2020 - 2039          | 1074.7            | 1213.2   | -225.3   | -86.8    | -17.3    | -6.7     | -17.3    | -6.7    |
| 2040 - 2059          | 1174.8            | 1030.5   | -125.2   | -269.5   | -9.6     | -20.7    | -9.6     | -20.7   |
| 2060 - 2079          | 1186.5            | 1071.2   | -113.5   | -228.8   | -8.7     | -17.6    | -8.7     | -17.6   |
| 2080 - 2099          | 1177.0            | 1246.7   | -123.0   | -53.3    | -9.5     | -4.1     | -9.5     | -4.1    |
| <b>MRI-ESM2-0</b>    |                   |          |          |          |          |          |          |         |
| 2020 - 2039          | 1264.7            | 1309.8   | -35.3    | 9.8      | -2.7     | 0.8      | -2.7     | 0.8     |
| 2040 - 2059          | 1194.6            | 1258.2   | -105.4   | -41.8    | -8.1     | -3.2     | -8.1     | -3.2    |
| 2060 - 2079          | 1196.9            | 1315.2   | -103.1   | 15.2     | -7.9     | 1.2      | -7.9     | 1.2     |
| 2080 - 2099          | 1127.3            | 1252.4   | -172.7   | -47.6    | -13.3    | -3.7     | -13.3    | -3.7    |
| <b>UKESM1-0-LL</b>   |                   |          |          |          |          |          |          |         |
| 2020 - 2039          | 1224.6            | 1241.1   | -75.4    | -58.9    | -5.8     | -4.5     | -5.8     | -4.5    |
| 2040 - 2059          | 1215.5            | 1332.6   | -84.5    | 32.6     | -6.5     | 2.5      | -6.5     | 2.5     |
| 2060 - 2079          | 1248.9            | 1488.7   | -51.1    | 188.7    | -3.9     | 14.5     | -3.9     | 14.5    |
| 2080 - 2099          | 1247.3            | 1570.0   | -52.7    | 270.0    | -4.1     | 20.8     | -4.1     | 20.8    |

Notes: GFDL-ESM4, Geophysical Fluid Dynamics Laboratory – Earth System Model version 4; IPSL-CM6A-LR, Institut Pierre-Simon Laplace – Climate Model version 6A – Low Resolution; MPI-ESM1-2-HR, Max Planck Institute – Earth System Model version 1.2 – High Resolution; MRI-ESM2-0, Meteorological Research Institute – Earth System Model version 2.0; and UKESM1-0-LL, United Kingdom Earth System Model version 1.0 – Low Resolution. SSP1-2.6 and SSP3-7.0 are Shared Socioeconomic Pathways (SSP) with numbers (2.6 and 7.0) referring to radiative forcing levels in watts per square meter (W/m<sup>2</sup>) reached by 2100 for each SSP, respectively and % is percentage.

### 312 3.3. Maximum Temperature

1 313 Generally, maximum temperatures in all five GCM models project an increase under SSP1-2.6 and  
2  
3 314 SSP3-7.0 climate scenarios (Table 5). Over the years, the temperature has been increasing with the  
4  
5 315 highest projected in the period 2040 – 2059 and 2060 – 2079 for all the climate scenarios per GCM  
6  
7 316 model (Table 5). Under the MPI-ESM1-2-HR model for periods 2060 – 2079 and 2080 – 2099, the  
8  
9 317 projected maximum temperature will be 32.1°C and 32.4°C, respectively while the UKESM1-0-LL  
10 318 model under similar periods and the climate scenarios projects relatively higher maximum temperatures  
11  
12 319 of 33.6°C and 35.0°C, respectively.

13  
14 320 For GFDL-ESM4, maximum temperatures increase consistently, with more substantial rises under  
15  
16 321 SSP3-7.0, reaching 2.6°C above baseline by 2080 – 2099 (8.7%). IPSL-CM6A-LR projects similar  
17  
18 322 patterns, with SSP3-7.0 showing a significant rise of 3.6°C (12.1%) by 2080 – 2099. MPI-ESM1-2-HR  
19 323 indicates moderate increases under SSP1-2.6 up to 2.4°C (7.9%), but less pronounced changes under  
20  
21 324 SSP3-7.0, suggesting potential regional variability. Also, MRI-ESM2-0 displays consistent warming  
22  
23 325 under SSP1-2.6, peaking at 2.9°C (9.6%) by 2080 – 2099, while SSP3-7.0 shows smaller increases,  
24  
25 326 possibly indicating mitigation effects. The UKESM1-0-LL shows the highest temperature increases,  
26  
27 327 particularly under SSP1-2.6, reaching 5.0°C (16.6%) by 2080 – 2099, suggesting a dramatic shift in  
28  
29 328 thermal conditions (Table 5). These projections highlight the significant warming expected, particularly  
30  
31 329 under high-emission climate scenarios, emphasizing the urgent need for robust soil water management  
32  
33 330 strategies.

33 331

332 **Table 5.** Changing in maximum temperature (°C) for the four periods under SSP1-2.6 and SSP3-7.0 climate scenarios.

| GCM models           | Climate Scenarios |          |          |          | Change   |          |          |          | %Change  |          |
|----------------------|-------------------|----------|----------|----------|----------|----------|----------|----------|----------|----------|
|                      | SSP1-2.6          | SSP3-7.0 | SSP1-2.6 | SSP3-7.0 | SSP1-2.6 | SSP3-7.0 | SSP1-2.6 | SSP3-7.0 | SSP1-2.6 | SSP3-7.0 |
| <b>GFDL-ESM4</b>     | SSP1-2.6          | SSP3-7.0 | SSP1-2.6 | SSP3-7.0 | SSP1-2.6 | SSP3-7.0 | SSP1-2.6 | SSP3-7.0 | SSP1-2.6 | SSP3-7.0 |
| Baseline             | 30                |          |          |          |          |          |          |          |          |          |
| 2020 - 2039          | 31.1              | 30.7     | 1.1      | 0.7      | 1.1      | 0.7      | 3.7      | 2.2      | 3.7      | 2.2      |
| 2040 - 2059          | 31.3              | 31.4     | 1.3      | 1.4      | 1.3      | 1.4      | 4.3      | 4.5      | 4.3      | 4.5      |
| 2060 - 2079          | 31.4              | 32.2     | 1.4      | 2.2      | 1.4      | 2.2      | 4.6      | 7.4      | 4.6      | 7.4      |
| 2080 - 2099          | 31.4              | 32.6     | 1.4      | 2.6      | 1.4      | 2.6      | 4.5      | 8.7      | 4.5      | 8.7      |
| <b>IPSL-CM6A-LR</b>  |                   |          |          |          |          |          |          |          |          |          |
| 2020 - 2039          | 31.2              | 31.0     | 1.2      | 1.0      | 1.2      | 1.0      | 4.1      | 3.4      | 4.1      | 3.4      |
| 2040 - 2059          | 31.4              | 31.8     | 1.4      | 1.8      | 1.4      | 1.8      | 4.6      | 6.1      | 4.6      | 6.1      |
| 2060 - 2079          | 31.3              | 32.6     | 1.3      | 2.6      | 1.3      | 2.6      | 4.2      | 8.8      | 4.2      | 8.8      |
| 2080 - 2099          | 31.2              | 33.6     | 1.2      | 3.6      | 1.2      | 3.6      | 4.1      | 12.1     | 4.1      | 12.1     |
| <b>MPI-ESM1-2-HR</b> |                   |          |          |          |          |          |          |          |          |          |
| 2020 - 2039          | 30.6              | 31.0     | 0.6      | 1.0      | 0.6      | 1.0      | 2.1      | 3.2      | 2.1      | 3.2      |
| 2040 - 2059          | 31.6              | 30.9     | 1.6      | 0.9      | 1.6      | 0.9      | 5.4      | 3.1      | 5.4      | 3.1      |
| 2060 - 2079          | 32.1              | 30.9     | 2.1      | 0.9      | 2.1      | 0.9      | 7.1      | 3.1      | 7.1      | 3.1      |
| 2080 - 2099          | 32.4              | 30.8     | 2.4      | 0.8      | 2.4      | 0.8      | 7.9      | 2.5      | 7.9      | 2.5      |
| <b>MRI-ESM2-0</b>    |                   |          |          |          |          |          |          |          |          |          |
| 2020 - 2039          | 30.3              | 30.8     | 0.3      | 0.8      | 0.3      | 0.8      | 0.9      | 2.6      | 0.9      | 2.6      |
| 2040 - 2059          | 31.3              | 31.3     | 1.3      | 1.3      | 1.3      | 1.3      | 4.4      | 4.2      | 4.4      | 4.2      |
| 2060 - 2079          | 32.1              | 31.5     | 2.1      | 1.5      | 2.1      | 1.5      | 7.1      | 4.9      | 7.1      | 4.9      |
| 2080 - 2099          | 32.9              | 31.5     | 2.9      | 1.5      | 2.9      | 1.5      | 9.6      | 4.9      | 9.6      | 4.9      |
| <b>UKESM1-0-LL</b>   |                   |          |          |          |          |          |          |          |          |          |
| 2020 - 2039          | 31.7              | 31.6     | 1.7      | 1.6      | 1.7      | 1.6      | 5.7      | 5.3      | 5.7      | 5.3      |
| 2040 - 2059          | 32.6              | 32.3     | 2.6      | 2.3      | 2.6      | 2.3      | 8.8      | 7.7      | 8.8      | 7.7      |
| 2060 - 2079          | 33.6              | 32.4     | 3.6      | 2.4      | 3.6      | 2.4      | 12.0     | 8.1      | 12.0     | 8.1      |
| 2080 - 2099          | 35.0              | 32.5     | 5.0      | 2.5      | 5.0      | 2.5      | 16.6     | 8.3      | 16.6     | 8.3      |

333 Notes: GFDL-ESM4, Geophysical Fluid Dynamics Laboratory – Earth System Model version 4; IPSL-CM6A-LR, Institut Pierre-Simon Laplace – Climate Model version 6A  
334 – Low Resolution; MPI-ESM1-2-HR, Max Planck Institute – Earth System Model version 1.2 – High Resolution; MRI-ESM2-0, Meteorological Research Institute – Earth  
335 System Model version 2.0; and UKESM1-0-LL, United Kingdom Earth System Model version 1.0 – Low Resolution. SSP1-2.6 and SSP3-7.0 are Shared Socioeconomic  
336 Pathways (SSP) with numbers (2.6 and 7.0) referring to the radiative forcing levels in watts per square meter (W/m<sup>2</sup>) reached by 2100 for each SSP, respectively, °C is degrees  
337 Celsius and % is percentage.

### 338 3.4. Minimum Temperature

1  
2 339 Generally, all GCM models project minimum temperature change under the SSP1-2.6 and SSP3-7.0  
3 340 climate scenarios compared to the baseline minimum temperature conditions. The models show  
4 341 substantial increases from the baseline of 15°C (Table 6). By 2080 – 2099, the minimum temperature  
5 342 rises range from 6.2°C – 8.6°C under SSP1-2.6 and 8.3°C – 10.3°C under SSP3-7.0, indicating  
6 343 significant warming. The highest increase is projected by UKESM1-0-LL, particularly under SSP3-7.0,  
7 344 with a 10.3°C rise, reflecting a 69.0% change from the baseline climate conditions. Such temperature  
8 345 increases could affect agricultural practices, maize yield, and stress tolerance, necessitating adaptive  
9 346 strategies to mitigate negative impacts on food production.

10 347 Over the years these temperatures are projected to rise gradually in all periods. From the results  
11 348 illustrated in Table 6, It can be expected that there will be no decrease in minimum temperature as the  
12 349 future period under SSP1-2.6 and SSP3-7.0 climate scenarios project increase. The change in minimum  
13 350 temperature for the period 2080 – 2099 is relatively more significant under MRI-ESM2-0 by 8.5% and  
14 351 UKESM1-0-LL by 7.4% for SSP1-2.6 and 10.3% for SSP3-7.0, respectively. The slightly lowest  
15 352 temperatures are observed in the period 2020 – 2039 under all climate scenarios (Table 6).

1  
2  
3  
4  
5  
6  
7  
8  
9  
10  
11  
12  
13  
14  
15  
16  
17  
18  
19  
20  
21  
22  
23  
24  
25  
26  
27  
28  
29  
30  
31  
32  
33  
34  
35  
36  
37  
38  
39  
40  
41  
42  
43  
44  
45  
46  
47  
48  
49  
50  
51  
52  
53  
54  
55  
56  
57  
58  
59  
60  
61  
62  
63  
64  
65

**Table 6.** Changing in minimum temperature (°C) for the four periods under SSP1-2.6 and SSP3-7.0 climate scenarios.

| GCM models           | Climate Scenarios |          |          |          | Change   |          | %Change  |          |
|----------------------|-------------------|----------|----------|----------|----------|----------|----------|----------|
|                      | SSP1-2.6          | SSP3-7.0 | SSP1-2.6 | SSP3-7.0 | SSP1-2.6 | SSP3-7.0 | SSP1-2.6 | SSP3-7.0 |
| <b>GFDL-ESM4</b>     |                   |          |          |          |          |          |          |          |
| Baseline             | 15                |          |          |          |          |          |          |          |
| 2020 - 2039          | 21.3              | 21.5     | 6.3      | 6.5      | 41.9     | 43.3     |          |          |
| 2040 - 2059          | 21.2              | 22.1     | 6.2      | 7.1      | 41.6     | 47.3     |          |          |
| 2060 - 2079          | 21.3              | 23.0     | 6.3      | 8.0      | 41.9     | 53.3     |          |          |
| 2080 - 2099          | 21.2              | 23.6     | 6.2      | 8.6      | 41.5     | 57.4     |          |          |
| <b>IPSL-CM6A-LR</b>  |                   |          |          |          |          |          |          |          |
| 2020 - 2039          | 21.0              | 21.1     | 6.0      | 6.1      | 40.0     | 40.6     |          |          |
| 2040 - 2059          | 21.5              | 22.4     | 6.5      | 7.4      | 43.1     | 49.3     |          |          |
| 2060 - 2079          | 21.6              | 23.7     | 6.6      | 8.7      | 43.8     | 57.7     |          |          |
| 2080 - 2099          | 21.5              | 25.1     | 6.5      | 10.1     | 43.5     | 67.3     |          |          |
| <b>MPI-ESM1-2-HR</b> |                   |          |          |          |          |          |          |          |
| 2020 - 2039          | 21.0              | 20.8     | 6.0      | 5.8      | 39.8     | 38.4     |          |          |
| 2040 - 2059          | 21.1              | 22.1     | 6.1      | 7.1      | 40.5     | 47.1     |          |          |
| 2060 - 2079          | 21.1              | 22.8     | 6.1      | 7.8      | 40.6     | 52.0     |          |          |
| 2080 - 2099          | 20.9              | 23.3     | 5.9      | 8.3      | 39.4     | 55.0     |          |          |
| <b>MRI-ESM2-0</b>    |                   |          |          |          |          |          |          |          |
| 2020 - 2039          | 20.8              | 20.8     | 5.8      | 5.8      | 38.4     | 38.4     |          |          |
| 2040 - 2059          | 21.7              | 21.7     | 6.7      | 6.7      | 44.5     | 44.5     |          |          |
| 2060 - 2079          | 22.6              | 22.6     | 7.6      | 7.6      | 50.9     | 50.9     |          |          |
| 2080 - 2099          | 23.5              | 23.5     | 8.5      | 8.5      | 56.5     | 56.5     |          |          |
| <b>UKESM1-0-LL</b>   |                   |          |          |          |          |          |          |          |
| 2020 - 2039          | 21.4              | 21.6     | 6.4      | 6.6      | 43.0     | 44.0     |          |          |
| 2040 - 2059          | 22.1              | 22.6     | 7.1      | 7.6      | 47.6     | 50.9     |          |          |
| 2060 - 2079          | 22.3              | 23.7     | 7.3      | 8.7      | 48.7     | 58.3     |          |          |
| 2080 - 2099          | 22.4              | 25.3     | 7.4      | 10.3     | 49.1     | 69.0     |          |          |

Notes: GFDL-ESM4, Geophysical Fluid Dynamics Laboratory – Earth System Model version 4; IPSL-CM6A-LR, Institut Pierre-Simon Laplace – Climate Model version 6A – Low Resolution; MPI-ESM1-2-HR, Max Planck Institute – Earth System Model version 1.2 – High Resolution; MRI-ESM2-0, Meteorological Research Institute – Earth System Model version 2.0; and UKESM1-0-LL, United Kingdom Earth System Model version 1.0 – Low Resolution. SSP1-2.6 and SSP3-7.0 are Shared Socioeconomic Pathways (SSP) with numbers (2.6 and 7.0) as the radiative forcing levels in watts per square meter (W/m<sup>2</sup>) reached by 2100 for each SSP, respectively, °C is degrees Celsius and % is percentage.

### 359 3.5. Projected impacts of SWMPs on maize grain yield

1  
2 360 Overall, simulations from the GCM climate models (GFDL-ESM4, IPSL-CM6A-LR, MPI-ESM1-2-  
3 361 HR, MRI-ESM2-0, and UKESM1-0-LL) did not show statistical significance ( $P > 0.05$ ) for soil water  
4 362 management practices (SWMPs) and maize grain yield. However, projected increases in maize yield  
5 363 are observed for different time periods (2020 – 2039, 2040 – 2059, 2060 – 2079, and 2080 – 2099)  
6 364 under various climate scenarios (Fig. 4).

7  
8  
9  
10  
11 365 The different GCM models exhibit considerable variation in their maize yield projections. For example,  
12 366 the MPI-ESM1-2-HR model frequently predicts decreases in yield (e.g., -15.6% for 2020 – 2039), while  
13 367 other models, such as UKESM1-0-LL, project increases. This variability is not consistent across all  
14 368 scenarios, as some models, like GFDL-ESM4, shift between positive and negative yield projections  
15 369 depending on the climate scenario.

16  
17  
18  
19  
20 370 There are significant differences in yield outcomes between the low and high emission scenarios. Under  
21 371 SSP1-2.6, most models predict an increase in maize yield when mulching is applied, although some  
22 372 reductions are observed (e.g., MPI-ESM1-2-HR). Conversely, under the SSP3-7.0 scenario, yield  
23 373 projections tend to be more variable, with GFDL-ESM4 consistently projecting decreases across most  
24 374 treatments.

25  
26  
27  
28  
29 375 Mulching thickness plays a crucial role in determining yield outcomes. Thicker mulching layers (4 cm  
30 376 and 6 cm) generally result in higher yields compared to conventional practices or thinner mulching  
31 377 treatments like the 2 cm. The impact of mulching thickness varies slightly across different climate  
32 378 scenarios, but its positive effect is more pronounced under SSP1-2.6. For instance, a 6 cm mulch  
33 379 thickness consistently results in yield increases across most models, except under more extreme  
34 380 conditions like SSP3-7.0, where reductions are seen, particularly with the GFDL-ESM4 model.

35  
36  
37  
38  
39  
40 381 Therefore, the interaction between climate models, scenarios, and mulching thickness in Fig. 4 greatly  
41 382 influences maize yield projections, with thicker mulching often providing better yield outcomes,  
42 383 especially in less extreme climate

43  
44  
45  
46 384

47 385

48  
49 386

50  
51 387

52  
53 388

54  
55

56

57

58

59

60

61  
62  
63  
64  
65

1  
2  
3  
4  
5  
6  
7  
8  
9  
10  
11  
12  
13  
14  
15  
16  
17  
18  
19  
20  
21  
22  
23  
24  
25  
26  
27  
28  
29  
30  
31  
32  
33  
34  
35  
36  
37  
38  
39  
40  
41  
42  
43  
44  
45  
46  
47  
48  
49  
50  
51  
52  
53  
54  
55  
56  
57  
58  
59  
60  
61  
62  
63  
64  
65

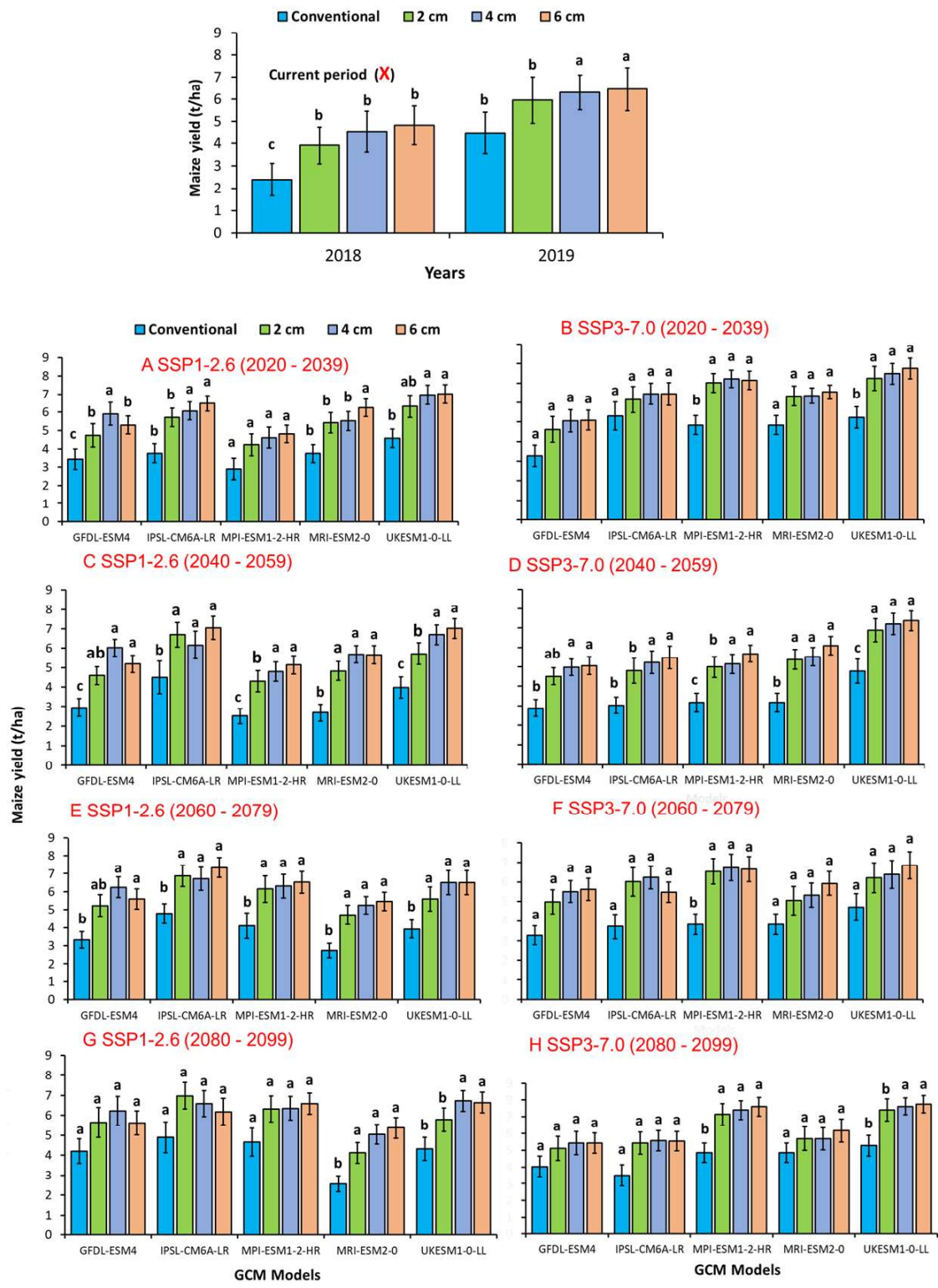


**Fig. 4.** Maize grain yield with SWMP practices for various time periods and climate scenarios. The graphs A – H present yields for the scenarios SSP1-2.6, and SSP3-7.0. To compare the current period with future effects of selected SWMPs, yield of the current period (2018 – 2019) with the same treatments (C, control or conventional, 2 cm thick, 4 cm thick, and 6 cm thick for straw mulches).

### 394 3.6. Projected maize evapotranspiration (ET)

1 395 Table 7 illustrates changes in maize ET under different climate models (GFDL-ESM4, IPSL-CM6A-  
2 396 LR, MPI-ESM1-2-HR, MRI-ESM2-0, and UKESM1-0-LL) with respective climate change scenarios  
3 397 (SSP1-2.6 and SSP3-7.0) from 2020 – 2099. The baseline observed ET for the 2018 – 2019 period is  
4 398 given for conventional practice (C) and three mulch thicknesses (2 cm, 4 cm, and 6 cm), showing values  
5 399 between 412 mm and 485 mm. All models generally project significant reductions in ET across both  
6  
7  
8  
9  
10 400 climate change scenarios and all mulch treatments.

11  
12 401 The highest reductions in ET are generally observed under conventional practice (C) across most  
13 402 models and scenarios. Mulch treatments (2 cm, 4 cm, and 6 cm) tend to moderate the reductions in ET  
14 403 compared to conventional practice, although reductions are still significant. The SSP1-2.6 shows  
15 404 slightly higher reductions in ET compared to SSP3-7.0 in several instances.

16  
17  
18  
19 405 Under SSP1-2.6, all models show substantial reductions in ET across all treatments (Table 7). The  
20 406 GFDL-ESM4 model shows significant ET reductions of -81.3% for conventional practice and -64.4%  
21 407 for 6 cm mulch thickness. Similarly, SSP3-7.0 also shows considerable ET reductions under selected  
22 408 SWMPs practices. The MRI-ESM2-0 model reduces ET by -66.9% for conventional practice and -  
23 409 74.0% for 6 cm mulch thickness. This indicates that, without significant mitigation efforts, climate  
24  
25  
26  
27 410 change will still lead to substantial decreases in ET, potentially impacting maize yield.

28 411

29 412

30  
31  
32  
33  
34  
35  
36  
37  
38  
39  
40  
41  
42  
43  
44  
45  
46  
47  
48  
49  
50  
51  
52  
53  
54  
55  
56  
57  
58  
59  
60  
61  
62  
63  
64  
65

**Table 7.** Changing in maize ET (mm) SSP1-2.6 and SSP3-7.0 climate scenarios.

| GCM models           | Observed ET (2018 – 2019) |          | Climate Scenarios (2018 – 2099) |          |          |          | Change in ET |          | % Change in ET |  |
|----------------------|---------------------------|----------|---------------------------------|----------|----------|----------|--------------|----------|----------------|--|
|                      | Baseline                  | SSP1-2.6 | SSP3-7.0                        | SSP1-2.6 | SSP3-7.0 | SSP1-2.6 | SSP3-7.0     | SSP1-2.6 | SSP3-7.0       |  |
| <b>GFDL-ESM4</b>     |                           |          |                                 |          |          |          |              |          |                |  |
| C                    | 485.0                     | 90.6     | 152.5                           | -394.4   | -332.5   | -81.3    | -68.6        |          |                |  |
| 2 cm                 | 468.0                     | 102.0    | 217.7                           | -366.0   | -250.3   | -78.2    | -53.5        |          |                |  |
| 4 cm                 | 417.0                     | 123.7    | 92.1                            | -293.3   | -324.9   | -70.3    | -77.9        |          |                |  |
| 6 cm                 | 412.0                     | 146.7    | 101.0                           | -265.3   | -311.0   | -64.4    | -75.5        |          |                |  |
| <b>IPSL-CM6A-LR</b>  |                           |          |                                 |          |          |          |              |          |                |  |
| C                    | 485.0                     | 101.2    | 197.2                           | -383.8   | -287.8   | -79.1    | -59.3        |          |                |  |
| 2 cm                 | 468.0                     | 119.1    | 114.9                           | -348.9   | -353.1   | -74.6    | -75.4        |          |                |  |
| 4 cm                 | 417.0                     | 164.3    | 98.3                            | -252.7   | -318.7   | -60.6    | -76.4        |          |                |  |
| 6 cm                 | 412.0                     | 150.0    | 112.0                           | -262.0   | -300.0   | -63.6    | -72.8        |          |                |  |
| <b>MPI-ESM1-2-HR</b> |                           |          |                                 |          |          |          |              |          |                |  |
| C                    | 485.0                     | 91.2     | 168.9                           | -393.8   | -316.1   | -81.2    | -65.2        |          |                |  |
| 2 cm                 | 468.0                     | 100.6    | 97.3                            | -367.4   | -370.7   | -78.5    | -79.2        |          |                |  |
| 4 cm                 | 417.0                     | 133.1    | 105.5                           | -283.9   | -311.5   | -68.1    | -74.7        |          |                |  |
| 6 cm                 | 412.0                     | 154.1    | 104.4                           | -257.9   | -307.6   | -62.6    | -74.7        |          |                |  |
| <b>MRI-ESM2-0</b>    |                           |          |                                 |          |          |          |              |          |                |  |
| C                    | 485.0                     | 80.3     | 160.7                           | -404.7   | -324.3   | -83.4    | -66.9        |          |                |  |
| 2 cm                 | 468.0                     | 94.0     | 95.3                            | -374.0   | -372.7   | -79.9    | -79.6        |          |                |  |
| 4 cm                 | 417.0                     | 126.3    | 105.9                           | -290.7   | -311.1   | -69.7    | -74.6        |          |                |  |
| 6 cm                 | 412.0                     | 146.6    | 107.3                           | -265.4   | -304.7   | -64.4    | -74.0        |          |                |  |
| <b>UKESM1-0-LL</b>   |                           |          |                                 |          |          |          |              |          |                |  |
| C                    | 485.0                     | 121.0    | 192.6                           | -364.0   | -292.4   | -75.1    | -60.3        |          |                |  |
| 2 cm                 | 468.0                     | 137.7    | 137.2                           | -330.3   | -330.8   | -70.6    | -70.7        |          |                |  |
| 4 cm                 | 417.0                     | 152.0    | 134.5                           | -265.0   | -282.5   | -63.5    | -67.7        |          |                |  |
| 6 cm                 | 412.0                     | 184.6    | 149.7                           | -227.4   | -262.3   | -55.2    | -63.7        |          |                |  |

Notes: GFDL-ESM4, Geophysical Fluid Dynamics Laboratory – Earth System Model version 4; IPSL-CM6A-LR, Institut Pierre-Simon Laplace – Climate Model version 6A – Low Resolution; MPI-ESM1-2-HR, Max Planck Institute – Earth System Model version 1.2 – High Resolution; MRI-ESM2-0, Meteorological Research Institute – Earth System Model version 2.0; and UKESM1-0-LL, United Kingdom Earth System Model version 1.0 – Low Resolution. SSP1-2.6 and SSP3-7.0 are Shared Socioeconomic Pathways (SSP), numbers (2.6 and 7.0) refer to the radiative forcing levels in watts per square meter (W/m<sup>2</sup>) reached by 2100 for each SSP, respectively and % is percentage. C, control or conventional, 2 cm thick, 4 cm thick, 6 cm thick for straw mulches and ET, Evapotranspiration.

### 420 3.7. Water Use Efficiency

1 421 Across all GCMs and SWMPs, there is a substantial increase in maize water use efficiency (WUE)  
2  
3 422 under both climate scenarios of SSP1-2.6 and SSP3-7.0 (Table 8). This indicates that, despite the  
4  
5 423 challenges posed by climate change, maize can potentially become more water-efficient. The baseline  
6  
7 424 WUE values, observed from 2018 – 2019, serve as a reference point for assessing future changes for  
8  
9 425 two climate scenarios. Under both climate scenarios, there is a substantial increase in WUE across all  
10 426 GCMs and SWMPs, indicating that maize could potentially become more water-efficient despite the  
11  
12 427 challenges posed by climate change. For example, the GFDL-ESM4 model projects an increase in WUE  
13 428 of 260% for conventional practices under SSP1-2.6 and 454% for 6 cm mulch thickness. Similar trends  
14  
15 429 are observed with IPSL-CM6A-LR, where the 4 cm mulch thickness shows an increase of 670% for  
16  
17 430 SSP1-2.6 and 761% under SSP3-7.0.

18 431

20 432 The MPI-ESM1-2-HR model indicates a WUE increase of 239.5% for conventional practice under  
21  
22 433 SSP1-2.6 and 302.5% for SSP3-7.0, with the highest increase noted for the 4 cm mulch thickness, which  
23  
24 434 rises by 690.5% under SSP1-2.6 and 805% with SSP3-7.0. The MRI-ESM2-0 model shows significant  
25 435 WUE increases across all practices, with the 4 cm mulch thickness experiencing a rise of 680% under  
26  
27 436 SSP1-2.6 and 769% under SSP3-7.0, while the 6 cm mulch also shows substantial improvements. The  
28  
29 437 UKESM1-0-LL model projects notable WUE increases across all SWMPs, with the 4 cm mulch  
30 438 thickness showing the highest increase of 805.5% under SSP1-2.6 and 877.5% for SSP3-7.0,  
31  
32 439 respectively marking the strongest potential for water efficiency improvements among the models.

33 440

35 441

36  
37  
38  
39  
40  
41  
42  
43  
44  
45  
46  
47  
48  
49  
50  
51  
52  
53  
54  
55  
56  
57  
58  
59  
60  
61  
62  
63  
64  
65

**Table 8.** Changing in WUE ( $\text{kg m}^{-3}$ ) under SSP1-2.6 and SSP3-7.0 climate scenarios.

| GCM models           | Observed biomass<br>(2018 – 2019) | Climate Scenarios (2018 – 2099) |          |          |          |          |          | Change in<br>WUE |          |          |  |  |  |
|----------------------|-----------------------------------|---------------------------------|----------|----------|----------|----------|----------|------------------|----------|----------|--|--|--|
|                      |                                   | Baseline                        | SSP1-2.6 | SSP3-7.0 | SSP1-2.6 | SSP3-7.0 | SSP1-2.6 | SSP3-7.0         | SSP1-2.6 | SSP3-7.0 |  |  |  |
| <b>GFDL-ESM4</b>     |                                   |                                 |          |          |          |          |          |                  |          |          |  |  |  |
| C                    | 0.20                              | 0.72                            | 0.72     | 0.72     | 0.52     | 0.52     | 0.52     | 0.52             | 260.0    | 258.0    |  |  |  |
| 2 cm                 | 0.30                              | 1.26                            | 1.18     | 1.18     | 0.96     | 0.88     | 0.88     | 0.88             | 318.3    | 294.0    |  |  |  |
| 4 cm                 | 0.20                              | 1.72                            | 1.56     | 1.56     | 1.52     | 1.36     | 1.36     | 1.36             | 760.0    | 677.5    |  |  |  |
| 6 cm                 | 0.30                              | 1.66                            | 1.66     | 1.66     | 1.36     | 1.36     | 1.36     | 1.36             | 454.0    | 454.7    |  |  |  |
| <b>IPSL-CM6A-LR</b>  |                                   |                                 |          |          |          |          |          |                  |          |          |  |  |  |
| C                    | 0.20                              | 0.77                            | 0.72     | 0.72     | 0.57     | 0.52     | 0.52     | 0.52             | 286.0    | 260.0    |  |  |  |
| 2 cm                 | 0.30                              | 1.64                            | 1.35     | 1.35     | 1.34     | 1.05     | 1.05     | 1.05             | 446.0    | 351.0    |  |  |  |
| 4 cm                 | 0.20                              | 1.54                            | 1.72     | 1.72     | 1.34     | 1.52     | 1.52     | 1.52             | 670.0    | 761.0    |  |  |  |
| 6 cm                 | 0.30                              | 2.08                            | 1.79     | 1.79     | 1.78     | 1.49     | 1.49     | 1.49             | 593.3    | 495.0    |  |  |  |
| <b>MPI-ESM1-2-HR</b> |                                   |                                 |          |          |          |          |          |                  |          |          |  |  |  |
| C                    | 0.20                              | 0.68                            | 0.81     | 0.81     | 0.48     | 0.61     | 0.61     | 0.61             | 239.5    | 302.5    |  |  |  |
| 2 cm                 | 0.30                              | 1.22                            | 1.47     | 1.47     | 0.92     | 1.17     | 1.17     | 1.17             | 307.7    | 390.3    |  |  |  |
| 4 cm                 | 0.20                              | 1.58                            | 1.81     | 1.81     | 1.38     | 1.61     | 1.61     | 1.61             | 690.5    | 805.0    |  |  |  |
| 6 cm                 | 0.30                              | 1.79                            | 1.92     | 1.92     | 1.49     | 1.62     | 1.62     | 1.62             | 496.7    | 539.0    |  |  |  |
| <b>MRI-ESM2-0</b>    |                                   |                                 |          |          |          |          |          |                  |          |          |  |  |  |
| C                    | 0.20                              | 0.60                            | 0.81     | 0.81     | 0.40     | 0.61     | 0.61     | 0.61             | 199.0    | 302.5    |  |  |  |
| 2 cm                 | 0.30                              | 1.20                            | 1.43     | 1.43     | 0.90     | 1.13     | 1.13     | 1.13             | 298.7    | 375.7    |  |  |  |
| 4 cm                 | 0.20                              | 1.56                            | 1.74     | 1.74     | 1.36     | 1.54     | 1.54     | 1.54             | 680.0    | 769.0    |  |  |  |
| 6 cm                 | 0.30                              | 1.71                            | 1.89     | 1.89     | 1.41     | 1.59     | 1.59     | 1.59             | 470.3    | 530.7    |  |  |  |
| <b>UKESM1-0-LL</b>   |                                   |                                 |          |          |          |          |          |                  |          |          |  |  |  |
| C                    | 0.20                              | 0.90                            | 1.07     | 1.07     | 0.70     | 0.87     | 0.87     | 0.87             | 350.0    | 435.5    |  |  |  |
| 2 cm                 | 0.30                              | 1.41                            | 1.66     | 1.66     | 1.11     | 1.36     | 1.36     | 1.36             | 370.0    | 453.0    |  |  |  |
| 4 cm                 | 0.20                              | 1.81                            | 1.96     | 1.96     | 1.61     | 1.76     | 1.76     | 1.76             | 805.5    | 877.5    |  |  |  |
| 6 cm                 | 0.30                              | 1.90                            | 2.06     | 2.06     | 1.60     | 1.76     | 1.76     | 1.76             | 533.0    | 587.0    |  |  |  |

Notes: GFDL-ESM4, Geophysical Fluid Dynamics Laboratory – Earth System Model version 4; IPSL-CM6A-LR, Institut Pierre-Simon Laplace – Climate Model version 6A – Low Resolution; MPI-ESM1-2-HR, Max Planck Institute – Earth System Model version 1.2 – High Resolution; MRI-ESM2-0, Meteorological Research Institute – Earth System Model version 2.0; and UKESM1-0-LL, United Kingdom Earth System Model version 1.0 – Low Resolution. SSP1-2.6 and SSP3-7.0 are Shared Socioeconomic Pathways (SSP), numbers (2.6 and 7.0) refer to the radiative forcing levels in watts per square meter ( $\text{W/m}^2$ ) reached by 2100 for each SSP, respectively and %, percentage. C, control or conventional, 2 cm thick, 4 cm thick, 6 cm thick for straw mulches and WUE, Water Use Efficiency in kilograms per cubic meter expressed as WUE ( $\text{kg m}^{-3}$ ).

449 **4. Discussion**

1 450

2 451 **4.1. Model performance**

3  
4  
5 452 The evaluation of the AquaCrop model using different soil water management practices (SWMPs) in  
6  
7 453 mid-western Uganda revealed significant insights into the model's accuracy and the effectiveness of  
8  
9 454 mulch thickness in improving maize yield predictions. This observation is consistent with findings from  
10 455 other studies (Ding et al., 2018; Keesstra et al., 2019; Li et al., 2018; Quan et al., 2024), which similarly  
11  
12 456 report increased maize yields with straw mulch. Similar trends of improved accuracy with thicker  
13  
14 457 mulching have been noted in studies using AquaCrop and other models, suggesting that mulch thickness  
15 458 enhances soil moisture retention, leading to better yield outcomes. The calibration and validation  
16  
17 459 phases of this study showed that AquaCrop model effectively simulates final maize biomass, with high  
18  
19 460 modeling efficiency (EF) values of 0.87 and 0.92, indicating a strong correlation between observed and  
20 461 simulated values.

21  
22  
23 462 The RMSE values further validated model's accuracy decreasing with increasing mulch thickness: were  
24  
25 463 2.56, 2.06, 1.38, and 1.16 t/ha for the control, 2 cm, 4 cm, and 6 cm mulch thicknesses, respectively.  
26 464 The 6 cm mulch treatment showed the lowest RMSE, indicating the smallest average prediction error  
27  
28 465 and the best model fit. This trend underscores how thicker mulch significantly enhances the model's  
29  
30 466 predictive accuracy by reducing soil water evaporation. Similar observations have been made in the  
31 467 past studies such as studies of Jia et al.(2021), which highlighted the insulating effect of mulch in  
32  
33 468 reducing soil water evaporation rates, particularly under maize production systems. Also, the PBias  
34  
35 469 analysis further confirmed that higher mulch thickness improves model accuracy, with progressively  
36  
37 470 smaller PBias values indicating minimal over or under-prediction. This suggests that thicker mulch  
38 471 applications lead to more reliable model predictions and greater accuracy.

39  
40  
41 472 While higher mulch thickness treatments generally improved the accuracy of the AquaCrop model in  
42  
43 473 simulating maize yield, not all observed effects were statistically significant ( $P > 0.05$ ). This may be  
44 474 attributed to limited inter-annual climatic variability during the study period and the inherent  
45  
46 475 uncertainties associated with future climate projections. Additionally, the relatively short time frame  
47  
48 476 and limited range of conditions may have constrained the robustness of the results. Future studies  
49 477 involving longer-term simulations and field experiments across diverse climatic conditions and  
50  
51 478 management scenarios would help enhance statistical power and reduce variability in evaluating the  
52  
53 479 impacts of mulch application.

54  
55 480

56  
57  
58 481

59  
60  
61  
62  
63  
64  
65

## 482 4.2. Climate trends, and maize yields

1  
2 483 The variations among GCM models underscore the importance of considering a range of scenarios and  
3  
4 484 models to capture the breadth of potential future conditions on maize productivity, corroborating  
5  
6 485 previous studies (Chemura et al., 2022b; Ruane et al., 2013; Tesfaye et al., 2017). Changes in maximum  
7  
8 486 and minimum temperatures will have profound implications for ecosystems, agriculture, water  
9  
10 487 resources, and human health, necessitating comprehensive adaptation and mitigation plans. Such  
11  
12 488 temperature increases could affect agricultural practices, maize yield, and stress tolerance, necessitating  
13  
14 489 adaptive strategies to mitigate negative impacts on food production.

15 490 In mid-western Uganda, annual precipitation sums are projected to change, with the magnitude and  
16  
17 491 direction of change depending on the emissions scenario and climate model. The majority of models  
18  
19 492 indicate an increase in future precipitation, potentially substantial under the high emissions scenario,  
20  
21 493 though variability exists between models (Chemura et al., 2019; Jägermeyr et al., 2021). Some models  
22  
23 494 in this study show increases in precipitation with higher intensity and frequency in the future compared  
24  
25 495 to current and historical scenarios.

26 496 The GFDL-ESM4 model projected consistent decreases in precipitation under both scenarios until 2080  
27  
28 497 – 2099, with potential stabilization indicated by a smaller decrease under SSP3-7.0. Conversely, the  
29  
30 498 UKESM1-0-LL model projected significant increases in precipitation, particularly under SSP1-7.0,  
31  
32 499 suggesting regional variability and the influence of different emission scenarios.

33  
34 500 Under the SSP1-2.6 scenario, which represents a sustainable pathway with significant mitigation  
35  
36 501 efforts, results show varying changes in precipitation, with some models projecting increases and others  
37  
38 502 decreases, reflecting inherent uncertainties in climate projections. The SSP3-7.0 scenario, indicative of  
39  
40 503 a high-emission future with minimal climate policy interventions, generally shows more pronounced  
41  
42 504 changes in precipitation patterns, suggesting greater volatility and variability, which could have  
43  
44 505 significant implications for agricultural planning and water resource management. Climate models  
45  
46 506 project mixed signals of both wet and dry conditions in mid-western Uganda over the 21<sup>st</sup> century,  
47  
48 507 affecting soil water management practices and maize yield.

49 508 Maximum and minimum temperatures are projected to increase across all GCMs and scenarios.  
50  
51 509 Projected increases in maximum temperature range from 0.8°C to 3.6°C under SSP1-2.6 and up to  
52  
53 510 8.7°C under SSP3-7.0. These significant temperature increases highlight potential stress on maize crops  
54  
55 511 and the need for adaptive strategies. Similarly, minimum temperatures are projected to rise, with  
56  
57 512 increases ranging from 6.2°C to 10.3°C by 2080 – 2099, indicating a substantial warming trend that  
58  
59 513 could impact crop growth and stress tolerance.

### 514 4.3. Soil water management practices and maize productivity

1 515 The findings of this study emphasize the significant impacts of climate change on soil water  
2 516 management practices (SWMPs) and their subsequent influence on maize productivity under rainfed  
3 517 conditions. Our projections highlight that climate change alters precipitation patterns, which can  
4 518 substantially affect soil water availability and, consequently, maize yield. These changes necessitate  
5 519 adaptive strategies to mitigate potential adverse effects and enhance food security and environmental  
6 520 sustainability.

7 521 A key finding is the consistent improvement in water use efficiency (WUE) with the application of  
8 522 different SWMPs, particularly a 6 cm mulch thickness. This increase in WUE across various climate  
9 523 models suggests that mulching can play a crucial role in enhancing maize productivity and resilience to  
10 524 climate change. By improving soil moisture retention and reducing evaporation, mulching helps maize  
11 525 plants better withstand climatic stresses, thereby contributing to more sustainable agricultural practices.  
12 526 These results align with other research conducted in Uganda and similar environments like (Kassam et  
13 527 al., 2014; Siatwiinda et al., 2021), reported that effective soil water management is vital for coping with  
14 528 climate variability and improving maize yields. Our study builds on this by demonstrating the  
15 529 effectiveness of specific SWMPs in maintaining and improving maize productivity. Furthermore, the  
16 530 findings are consistent with past studies by Bu et al., (2013) and Zhang et al., (2020), which have shown  
17 531 that, various SWMPs, such as mulching, improve water retention and crop resilience across different  
18 532 regions and crops. For instance (Bu et al., 2013; Mupangwa et al., 2013; Okunade et al., 2020; Kader  
19 533 et al., 2019; Ullah et al., 2019; Zhang et al., 2020), highlights the effectiveness of mulching in diverse  
20 534 agricultural settings, showing that it can mitigate the impacts of climate change on crop yields by  
21 535 enhancing soil moisture and reducing temperature fluctuations. This supports our findings that  
22 536 mulching is a valuable practice for improving water use efficiency and crop productivity.

23 537 The discrepancy between the 6 cm mulch thickness for being optimal for maize grain yield and the 4 cm  
24 538 mulch thickness achieving the highest water use efficiency may be reflecting complementary  
25 539 relationship between productivity and efficiency under projected climate change. The 4 cm mulch  
26 540 thickness improves WUE across the GCMs, this may be due to a favourable balance of transpiration  
27 541 and evaporation, the 6 cm mulch thickness more consistently enhanced grain yield, particularly under  
28 542 the SSP1-2.6 scenario. This may be attributed to better soil moisture retention, moderated soil  
29 543 temperature, and improved root-zone conditions as corroborated by studies of Liu et al.(2017),  
30 544 Maharjan et al. (2018), Tian et al.( 2022), Wang et al., (202), Wang et al., (2019), and Zhao et al.  
31 545 (2022). The slightly lower WUE at 6 cm mulch is not indicative of inefficiency but results from  
32 546 increased total water uptake associated with higher biomass production. Thus, rather than being  
33 547 contradictory, these findings highlight a trade-off like, the 4 cm mulch optimizes per unit water  
34 548 efficiency, while the 6 cm mulch maximizes overall yield, making it the more effective choice for  
35 549 integrated soil and water management. Therefore, under changing climates, 6 cm straw mulch provides

550 a balanced strategy to enhance productivity while maintaining sustainable water use (Ullah et al., 2022;  
1 551 Zhang et al., 2017), supporting resilient agroecosystem development.  
2  
3

4 552 Also, the observed reductions in evapotranspiration (ET) across all climate models and mulch  
5 treatments (Table 7) align strongly with the substantial improvements in water use efficiency (WUE)  
6 553 reported in Table 8. This relationship highlights the role of reduced ET as a direct contributor to  
7 554 enhancing the WUE under future climate change scenarios, and this has been reported in previous  
8 555 studies (Huang et al., 2015; Zhao et al., 2022). Specifically, mulch reduces water losses which are non-  
9 556 productive to crops like evaporation and more water is directed in transpiration, hence a physiologically  
10 557 productive component of ET ( Wang et al., 2021). In the present study, the 4 cm and 6 cm straw mulches  
11 558 consistently reduce ET compared to the baseline, with the 4 cm mulch achieving the highest WUE in  
12 559 most GCMs and climate change scenarios. For instance, under the GFDL-ESM4 model with SSP1-2.6,  
13 560 there is a 70.3% ET reduction and a 760% increase in WUE for the 4 cm mulch thickness, which  
14 561 indicates a strong inverse relationship. Notably, while 6 cm mulch results in slightly less WUE than  
15 562 4 cm, it maintains greater yield due to higher overall water retention and improved microclimatic  
16 563 conditions similar to previous studies (Liu et al., 2014; Rahman et al., 2017). Therefore, these findings  
17 564 support the hypothesis that WUE gains stem from a more favourable partitioning of water fluxes, where  
18 565 mulching reduces total ET by significantly reducing and suppressing soil evaporation, thereby  
19 566 improving transpiration efficiency (El-Beltagi et al., 2022; Farzi et al., 2017; Y. Liu et al., 2017). Thus,  
20 567 application of mulching techniques in the progressive projected climate change should consider the  
21 568 scale of ET reduction and contribute to yield driven WUE gains.  
22  
23  
24  
25  
26  
27  
28  
29  
30  
31  
32  
33  
34  
35

36 570 However, the practical adoption of mulching faces several challenges. While the benefits of mulching  
37 571 are evident, its implementation involves labour and costs that can be prohibitive, particularly for farmers  
38 572 with large fields or limited resources. The availability of mulching materials to optimize the thickness  
39 573 and the additional labour required for application may be significant barriers. Farmers may be hesitant  
40 574 to adopt these practices due to these constraints, despite the potential yield improvements. Addressing  
41 575 these barriers is crucial for broader adoption and research into the cost-benefit ratios of mulching and  
42 576 other adaptation strategies is necessary to determine if the increased yield justifies the investment.  
43 577 Evaluating the economic viability and providing support for accessing materials and labour could  
44 578 enhance the adoption of effective SWMPs. The effectiveness of mulching as a SWMP for enhancing  
45 579 maize productivity in the face of climate change, practical considerations regarding its implementation  
46 580 must be addressed for future increased adoption. Future research should also focus on detailed cost-  
47 581 benefit analyses and strategies to overcome barriers to adoption, ensuring that the benefits of these  
48 582 adaptive practices can be realized in real-world agricultural settings.  
49  
50  
51  
52  
53  
54  
55  
56  
57

58 583  
59  
60  
61  
62  
63  
64  
65

584 **5. Conclusion**

1  
2 585 The results indicate that climate change, as projected by different GCMs and scenarios is expected to  
3 586 significantly impact maize productivity and, consequently, maize yield. While mulch thickness help  
4  
5 587 mitigate some of these impacts by reducing evapotranspiration, there is need for additional adaptive  
6  
7 588 measures in agriculture to sustain productivity in the face of climate change.  
8

9  
10 589 Also, the AquaCrop model demonstrated robust performance in simulating maize biomass under  
11  
12 590 different soil water management practices, with higher mulch thickness treatments significantly  
13 591 improving model accuracy. The findings emphasize the importance of mulch application in reducing  
14  
15 592 soil water evaporation and enhancing maize yield predictions. The model's ability to accurately simulate  
16  
17 593 biomass with different mulch thicknesses suggests its utility in optimizing soil water management  
18 594 strategies for improved agricultural productivity.  
19

20  
21 595 Future climate projections indicate significant challenges for maize production due to expected  
22  
23 596 decreases in precipitation and substantial increases in maximum and minimum temperatures. These  
24 597 changes underscore the urgency for adaptive strategies to mitigate the negative impacts on maize yields.  
25  
26 598 The variability among GCM projections also highlights the need for region-specific climate adaptation  
27  
28 599 plans.  
29

30  
31 600 In conclusion, the combination of effective soil water management practices, as evidenced by the  
32  
33 601 AquaCrop model simulations, and proactive soil water management practices will be crucial for  
34 602 sustaining maize production in the face of future climate challenges. Further research should focus on  
35  
36 603 refining model predictions and precision under varying climatic conditions and exploring additional  
37 604 soil and crop management practices to enhance resilience and productivity in maize farming systems.  
38  
39

40 **Acknowledgment**

41  
42 606 We acknowledge funding from the Agroecosystem 4CSA initiative, and we thank Meridel Murphy  
43  
44 607 Phillips at the NASA Goddard Institute for Space Studies for valuable contribution in providing the raw  
45 608 climate datasets and Professor Elias Fereres of IAS-CSIC, University of Cordoba for paper input  
46  
47 609 contributions.  
48  
49

50 **Declaration of Competing Interest**

51  
52  
53 611 The authors declare that they have no competing financial interests  
54  
55  
56  
57  
58  
59  
60  
61  
62  
63  
64  
65

612 **References**

- 1  
2 613  
3  
4 614 Araya, A., Hoogenboom, G., Luedeling, E., Hadgu, K.M., Kisekka, I., Martorano, L.G., 2015.  
5 615 Assessment of maize growth and yield using crop models under present and future climate in  
6 616 southwestern Ethiopia. *Agric. For. Meteorol.* 214–215, 252–265.  
7 617 <https://doi.org/10.1016/j.agrformet.2015.08.259>  
8  
9 618 Arumugam, P., Chemura, A., Aschenbrenner, P., Schaubberger, B., Gornott, C., 2023. Climate change  
10 619 impacts and adaptation strategies : An assessment on sorghum for Burkina Faso. *Eur. J. Agron.*  
11 620 142, 126655. <https://doi.org/10.1016/j.eja.2022.126655>  
12  
13 621 Ayanlade, A., Oluwaranti, A., Ayanlade, O.S., Borderon, M., Sterly, H., Sakdapolrak, P., Jegede,  
14 622 M.O., Weldemariam, L.F., Ayinde, A.F.O., 2022. Extreme climate events in sub-Saharan  
15 623 Africa : A call for improving agricultural technology transfer to enhance adaptive capacity 27.  
16  
17 624 Ayanlade, A., Radeny, M., Morton, J.F., Muchaba, T., 2018. Science of the Total Environment  
18 625 Rainfall variability and drought characteristics in two agro-climatic zones : An assessment of  
19 626 climate change challenges in Africa. *Sci. Total Environ.* 630, 728–737.  
20 627 <https://doi.org/10.1016/j.scitotenv.2018.02.196>  
21  
22 628 Biazin, B., Sterk, G., Temesgen, M., Abdulkedir, A., Stroosnijder, L., 2012. Rainwater harvesting and  
23 629 management in rainfed agricultural systems in sub-Saharan Africa – A review. *Phys. Chem.*  
24 630 *Earth* 47–48, 139–151. <https://doi.org/10.1016/j.pce.2011.08.015>  
25  
26 631 Boote, K., Makumbi, D., Robertson, R., Tesfaye, K., Gbegbelegbe, S., Cairns, J.E., Shiferaw, B.,  
27 632 Prasanna, B.M., Sonder, K., Boote, K., Makumbi, D., Robertson, R., 2015. Maize systems under  
28 633 climate change in sub-Saharan Africa. <https://doi.org/10.1108/IJCCSM-01-2014-0005>  
29  
30 634 Bu, L.D., Liu, J.L., Zhu, L., Luo, S.S., Chen, X.P., Li, S.Q., Lee Hill, R., Zhao, Y., 2013. The effects  
31 635 of mulching on maize growth, yield and water use in a semi-arid region. *Agric. Water Manag.*  
32 636 123, 71–78. <https://doi.org/10.1016/j.agwat.2013.03.015>  
33  
34 637 Chemura, A., Kutwayo, D., Hikwa, D., Gornott, C., 2022a. Climate change and cocoyam ( *Colocasia*  
35 638 *esculenta* ( L . ) Schott ) production : assessing impacts and potential adaptation strategies in  
36 639 Zimbabwe. *Mitig. Adapt. Strateg. Glob. Chang.* 27, 1–20. [https://doi.org/10.1007/s11027-022-](https://doi.org/10.1007/s11027-022-10014-9)  
37 640 10014-9  
38  
39 641 Chemura, A., Nangombe, S.S., Gleixner, S., Chinyoka, S., Gornott, C., 2022b. Changes in Climate  
40 642 Extremes and Their Effect on Maize ( *Zea mays* L . ) Suitability Over Southern Africa 4, 1–14.  
41 643 <https://doi.org/10.3389/fclim.2022.890210>  
42  
43 644 Chemura, A., Yalew, A.W., Gornott, C., Arumugam, P., 2019. Using yield projections from crop  
44 645 models to inform adaptation investments in Africa : An application to maize crop in Ghana 2–3.  
45 646 <https://doi.org/10.13140/RG.2.2.12838.37446>  
46  
47 647 Cucchi, M., Weedon, G.P., Amici, A., Bellouin, N., Lange, S., Schmied, H.M., Hersbach, H.,  
48 648 Buontempo, C., 2020. WFDE5 : bias-adjusted ERA5 reanalysis data for impact studies 60,  
49 649 2097–2120.  
50  
51 650 Demo, A. H., & Asefa Bogale, G. (2024). Enhancing crop yield and conserving soil moisture through  
52 651 mulching practices in dryland agriculture. *Frontiers in Agronomy*, 6, 1361697. [https://doi:](https://doi.org/10.3389/fagro.2024.1361697)  
53 652 10.3389/fagro.2024.1361697.  
54  
55 653 Dickerson, S., Cannon, M., Neill, B.O., 2021. Climate change risks to human development in sub-  
56 654 Saharan Africa : a review of the literature. *Clim. Dev.* 0, 1–19.  
57 655 <https://doi.org/10.1080/17565529.2021.1951644>  
58  
59 656 Ding, D., Zhao, Y., Feng, H., Hill, R.L., Chu, X., Zhang, T., He, J., 2018. Soil water utilization with  
60  
61  
62  
63  
64  
65

- 657 plastic mulching for a winter wheat-summer maize rotation system on the Loess Plateau of  
1 658 China. *Agric. Water Manag.* 201, 246–257. <https://doi.org/10.1016/j.agwat.2017.12.029>
- 2  
3 659 Doorenbos, Pruitt, 1977. Crop water requirements crop water requirements, *Irrigation and Drainage*  
4 660 paper. <https://doi.org/10.1002/aic.10277>
- 5  
6 661 El-Beltagi, H. S., Basit, A., Mohamed, H. I., Ali, I., Ullah, S., Kamel, E. A., & Ghazzawy, H. S.  
7 662 (2022). Mulching as a sustainable water and soil saving practice in agriculture: A  
8 663 review. *Agronomy*, 12(8), 1881. <https://doi.org/10.3390/agronomy12081881>
- 9  
10 664 Gupta, H.V., Sorooshian, S., Yapo, P.O., 1999. Status of Automatic Calibration for Hydrologic  
11 665 Models: Comparison with Multilevel Expert Calibration. *J. Hydrol. Eng.* 4, 135–143.  
12 666 [https://doi.org/10.1061/\(asce\)1084-0699\(1999\)4:2\(135\)](https://doi.org/10.1061/(asce)1084-0699(1999)4:2(135))
- 13  
14 667 FAOSTAT (2017). Land Use Statistics. Food and Agriculture Organization of the United Nations.  
15 668 Available at: <http://www.fao.org/faostat/en/#data>
- 16  
17 669 Farzi, R., Gholami, M., Baninasab, B., & Gheysari, M. (2017). Evaluation of different mulch materials  
18 670 for reducing soil surface evaporation in semi-arid region. *Soil Use and Management*, 33(1), 120–  
19 671 128. <https://doi.org/10.1111/sum.12325>
- 20  
21 672 Feng, Z., Miao, Q., Shi, H., Gonçalves, J. M., Li, X., Feng, W., & Yan, Y. (2025). AquaCrop model-  
22 673 based sensitivity analysis of soil salinity dynamics and productivity under climate change in  
23 674 sandy-layered farmland. *Agricultural Water Management*, 307, 109244.  
24 675 <https://doi.org/10.1016/j.agwat.2024.109244>.
- 25  
26 676 Harrison, L., Funk, C., & Peterson, P. (2019). Identifying changing precipitation extremes in Sub-  
27 677 Saharan Africa with gauge and satellite products. *Environmental Research Letters*, 14(8),  
28 678 085007.
- 29  
30 679 Hsiao, T.C., Heng, L., Steduto, P., Rojas-lara, B., Raes, D., Fereres, E., 2009. AquaCrop—The FAO  
31 680 Crop Model to Simulate Yield Response to Water: III. Parameterization and Testing for Maize.  
32 681 <https://doi.org/10.2134/agronj2008.0218s>
- 33  
34 682 Huang, M., Piao, S., Sun, Y., Ciais, P., Cheng, L., Mao, J., Poulter, B., Shi, X., Zeng, Z., & Wang, Y.  
35 683 (2015). Change in terrestrial ecosystem water-use efficiency over the last three decades. *Global*  
36 684 *Change Biology*, 21(6), 2366–2378. <https://doi.org/10.1111/gcb.12873>
- 37  
38 685 IPCC, 2021. Climate Change 2021: The Physical Science Basis - Summary for the Policymakers  
39 686 (Working Group I), *Climate Change 2021: The Physical Science Basis*.
- 40  
41 687 Jägermeyr, J., Müller, C., Ruane, A.C., Elliott, J., Balkovic, J., Castillo, O., Faye, B., Foster, I.,  
42 688 Folberth, C., Franke, J.A., Fuchs, K., Guarin, J.R., Heinke, J., Hoogenboom, G., Iizumi, T., Jain,  
43 689 A.K., Kelly, D., Khabarov, N., Lange, S., Lin, T.S., Liu, W., Mialyk, O., Minoli, S., Moyer, E.J.,  
44 690 Okada, M., Phillips, M., Porter, C., Rabin, S.S., Scheer, C., Schneider, J.M., Schyns, J.F.,  
45 691 Skalsky, R., Smerald, A., Stella, T., Stephens, H., Webber, H., Zabel, F., Rosenzweig, C., 2021.  
46 692 Climate impacts on global agriculture emerge earlier in new generation of climate and crop  
47 693 models. *Nat. Food* 2, 873–885. <https://doi.org/10.1038/s43016-021-00400-y>
- 49  
50 694 Jia, H., Chen, F., Zhang, C., Dong, J., Du, E., & Wang, L. (2022). High emissions could increase the  
51 695 future risk of maize drought in China by 60–70 %. *Science of the Total Environment*, 852(9),  
52 696 158474. <https://doi.org/10.1016/j.scitotenv.2022.158474>
- 53  
54 697 Jia, Q., Shi, H., Li, R., Miao, Q., Feng, Y., Wang, N., 2021. Evaporation of maize crop under mulch  
55 698 film and soil covered drip irrigation : field assessment and modelling on West Liaohe Plain ,  
56 699 China. *Agric. Water Manag.* 253, 106894. <https://doi.org/10.1016/j.agwat.2021.106894>
- 57  
58 700 Kader, M. A., Senge, M., Mojid, M. A., & Nakamura, K. (2017). Mulching type-induced soil  
59 701 moisture and temperature regimes and water use efficiency of soybean under rain-fed condition  
60 702 in central Japan. *International Soil and Water Conservation Research*, 5(4), 302–308.
- 61  
62  
63  
64  
65

- 703 <https://doi.org/10.1016/j.iswcr.2017.08.001>
- 1 704
- 2 705 Kaizzi, K.C., Byalebeka, J., Semalulu, O., Alou, I., Zimwanguyizza, W., Nansamba, A., Musinguzi,
- 3 706 P., Ebanyat, P., Hyuha, T., Wortmann, C.S., 2012. Maize Response to Fertilizer and Nitrogen
- 4 707 Use Efficiency in Uganda. <https://doi.org/10.2134/agronj2011.0181>
- 5
- 6 708 Karger, D.N., Lange, S., Hari, C., Reyer, C.P.O., Conrad, O., 2023. CHELSA-W5E5 : daily 1 km
- 7 709 meteorological forcing data for climate impact studies 2445–2464.
- 8
- 9 710 Kassam, A., Derpsch, R., Friedrich, T., 2014. Global achievements in soil and water conservation :
- 10 711 The case of Conservation Agriculture 1 Introduction. *Int. soil water Conserv. Res.* 2, 5–13.
- 11 712 [https://doi.org/10.1016/S2095-6339\(15\)30009-5](https://doi.org/10.1016/S2095-6339(15)30009-5)
- 12
- 13 713 Keesstra, S.D., Rodrigo-Comino, J., Novara, A., Giménez-Morera, A., Pulido, M., Di Prima, S.,
- 14 714 Cerdà, A., 2019. Straw mulch as a sustainable solution to decrease runoff and erosion in
- 15 715 glyphosate-treated clementine plantations in Eastern Spain. An assessment using rainfall
- 16 716 simulation experiments. *Catena* 174, 95–103. <https://doi.org/10.1016/j.catena.2018.11.007>
- 17
- 18 717 Kader, M. A., Singha, A., Begum, M. A., Jewel, A., Khan, F. H., & Khan, N. I. (2019). Mulching as
- 19 718 water-saving technique in dryland agriculture. *Bulletin of the National Research Centre*, 43(1), 1-
- 20 719 6. <https://doi.org/10.1186/s42269-019-0186-7>
- 21
- 22 720 Kikoyo, D.A., Nobert, J., 2016. Assessment of impact of climate change and adaptation strategies on
- 23 721 maize production in Uganda. *Phys. Chem. Earth* 93, 37–45.
- 24 722 <https://doi.org/10.1016/j.pce.2015.09.005>
- 25
- 26 723 Lamptey, S., Li, L., Xie, J., Coulter, A., 2020. Soil & Tillage Research Tillage system affects soil
- 27 724 water and photosynthesis of plastic-mulched maize on the semiarid Loess Plateau of China 196.
- 28 725 <https://doi.org/10.1016/j.still.2019.104479>
- 29
- 30 726 Lange, S., 2019. Trend-preserving bias adjustment and statistical downscaling with ISIMIP3BASD
- 31 727 (v1.0). *Geosci. Model Dev.* 12, 3055–3070. <https://doi.org/10.5194/gmd-12-3055-2019>
- 32
- 33 728 Li, Q., Li, H., Zhang, L., Zhang, S., Chen, Y., 2018. Field Crops Research Mulching improves yield
- 34 729 and water-use efficiency of potato cropping in China : A meta-analysis 221, 50–60.
- 35 730 <https://doi.org/10.1016/j.fcr.2018.02.017>
- 36
- 37 731 Lin, W., Liu, W., Xue, Q., 2016. Spring maize yield, soil water use and water use efficiency under
- 38 732 plastic film and straw mulches in the Loess Plateau. *Sci. Rep.* 6.
- 39 733 <https://doi.org/10.1038/srep38995>
- 40
- 41 734 Liu, H., Wang, X., Zhang, X., Zhang, L., Li, Y., & Huang, G. (2017). Evaluation on the responses of
- 42 735 maize (*Zea mays* L.) growth, yield and water use efficiency to drip irrigation water under mulch
- 43 736 condition in the Hetao irrigation District of China. *Agricultural Water Management*, 179, 144–
- 44 737 157. <https://doi.org/10.1016/j.agwat.2016.05.031>
- 45
- 46 738 Liu, J., Bu, L., Zhu, L., Luo, S., Chen, X., & Li, S. (2014). Optimizing Plant Density and Plastic Film
- 47 739 Mulch to Increase Maize Productivity and Water-Use Efficiency in Semiarid Areas. July.
- 48 740 <https://doi.org/10.2134/agronj13.0582>
- 49 741
- 50 742 Liu, Y., Hu, X., Zhang, Q., & Zheng, M. (2017). Improving agricultural water use efficiency: A
- 51 743 quantitative study of Zhangye City using the static CGE model with a ces water-land resources
- 52 744 account. *Sustainability (Switzerland)*, 9(2). <https://doi.org/10.3390/su9020308>
- 53 745 Lipper, L.,
- 54 746 Thornton, P., Campbell, B.M., Baedeker, T., Braimoh, A., Bwalya, M., Caron, P., Cattaneo, A.,
- 55 747 Garrity, D., Henry, K., Hottle, R., Jackson, L., Jarvis, A., Kossam, F., Mann, W., McCarthy, N.,
- 56 748 Meybeck, A., Neufeldt, H., Remington, T., Sen, P.T., Sessa, R., Shula, R., Tibu, A., Torquebiau,
- 57 749 E.F., 2014. Climate-smart agriculture for food security. *Nat. Clim. Chang.* 4, 1068–1072.
- 58
- 59 749 <https://doi.org/10.1038/NCLIMATE2437>
- 60
- 61
- 62
- 63
- 64
- 65

- 750 O'Neill, B.C., Tebaldi, C., van Vuuren, D.P., Eyring, V., Friedlingstein, P., Hurtt, G., Knutti, R.,  
1 751 Krieglner, E., Lamarque, J.F., Lowe, J., Meehl, G.A., Moss, R., Riahi, K., Sanderson, B.M., 2016.  
2 752 The scenario model intercomparison project (ScenarioMIP) for CMIP6. *Geosci. Model Dev.* 9,  
3 753 3461–3482. <https://doi.org/10.5194/gmd-9-3461-2016>,2016.  
4
- 5 754 Maharjan, G. R., Prescher, A. K., Nendel, C., Ewert, F., Mboh, C. M., Gaiser, T., & Seidel, S. J.  
6 755 (2018). Approaches to model the impact of tillage implements on soil physical and nutrient  
7 756 properties in different agro-ecosystem models. *Soil and Tillage Research*, 180(February), 210–  
8 757 221. <https://doi.org/10.1016/j.still.2018.03.009>  
9
- 10 758 Moriasi, D.N., Gitau, M.W., Pai, N., Daggupati, P., 2015. Hydrologic and water quality models:  
11 759 Performance measures and evaluation criteria. *Trans. ASABE* 58, 1763–1785.  
12 760 <https://doi.org/10.13031/trans.58.10715>.  
13
- 14 761 Mhlanga, B., 2021. The crucial role of mulch to enhance the stability and resilience of cropping  
15 762 systems in southern Africa.  
16
- 17 763 Mubiru, D.N., Radeny, M., Kyazze, F.B., Zziwa, A., Lwasa, J., Kinyangi, J., Mungai, C., 2018.  
18 764 Climate trends, risks and coping strategies in smallholder farming systems in Uganda. *Clim.*  
19 765 *Risk Manag.* 22, 4–21. <https://doi.org/10.1016/j.crm.2018.08.004>  
20
- 21 766 Mupangwa, W., Twomlow, S., Walker, S., 2013. Cumulative effects of reduced tillage and mulching  
22 767 on soil properties under semi-arid conditions. *J. Arid Environ.* 91, 45–52.  
23 768 <https://doi.org/10.1016/j.jaridenv.2012.11.007>  
24
- 25 769 Ngetich, K.F., Diels, J., Shisanya, C.A., Mugwe, J.N., Mucheru-muna, M., Mugendi, D.N., 2014.  
26 770 Catena Effects of selected soil and water conservation techniques on runoff, sediment yield and  
27 771 maize productivity under sub-humid and semi-arid conditions in Kenya. *Catena* 121, 288–296.  
28 772 <https://doi.org/10.1016/j.catena.2014.05.026>  
29
- 30 773 Okoboi, G. (2010). Of What Merit is Improved Inputs use in Uganda's Maize Productivity?.  
31
- 32 774 Okunade, D.A., Adekalu, K.O., Gowing, J.W., 2020. Effect of runoff management and soil  
33 775 conservation practices on the growth and yield of Maize (*Zea mays*) in a sub-humid agro-  
34 776 climatic zone of Ile-Ife, Nigeria. *IOP Conf. Ser. Earth Environ. Sci.* 445, 0–20.  
35 777 <https://doi.org/10.1088/1755-1315/445/1/012027>  
36
- 37 778 Ongoma, V., Chen, H., Gao, C., Nyongesa, A.M., Polong, F., 2018. Future changes in climate  
38 779 extremes over Equatorial East Africa based on CMIP5 multimodel ensemble. *Nat. Hazards* 90,  
39 780 901–920. <https://doi.org/10.1007/s11069-017-3079-9>  
40
- 41 781 Quan, H., Wu, L., Wang, B., Feng, H., 2024. Incorporating canopy radiation enhances the explanation  
42 782 of maize yield change and increases model accuracy under film mulching. *Eur. J. Agron.* 158,  
43 783 127198. <https://doi.org/10.1016/j.eja.2024.127198>  
44
- 45 784 Raes, D., Geerts, S., Kipkorir, E., Wellens, J., Sahli, A., 2006. Simulation of yield decline as a result  
46 785 of water stress with a robust soil water balance model. *Agric. Water Manag.* 81, 335–357.  
47 786 <https://doi.org/10.1016/j.agwat.2005.04.006>  
48
- 49 787 Rahman, T., Liu, X., Hussain, S., Ahmed, S., Chen, G., Yang, F., Chen, L., Du, J., Liu, W., & Yang,  
50 788 W. (2017). Water use efficiency and evapotranspiration in maize-soybean relay strip intercrop  
51 789 systems as affected by planting geometries. *PLoS ONE*, 12(6), 1–20.  
52 790 <https://doi.org/10.1371/journal.pone.0178332>  
53
- 54 791 Ruane, A.C., Cecil, L.D., Horton, R.M., Gordón, R., Mccollum, R., Brown, D., Killough, B.,  
55 792 Goldberg, R., Greeley, A.P., Rosenzweig, C., 2013. Agricultural and Forest Meteorology  
56 793 Climate change impact uncertainties for maize in Panama : Farm information , climate  
57 794 projections , and yield sensitivities. *Agric. For. Meteorol.* 170, 132–145.  
58 795 <https://doi.org/10.1016/j.agrformet.2011.10.015>  
59  
60  
61  
62  
63  
64  
65

- 796 Sawadogo H (2011) Using soil and water conservation techniques to rehabilitate degraded lands in  
1 797 Northwestern Burkina Faso. *Int J Agric Sustain* 9:120–128. [https://doi.org/10.3763/ijas.](https://doi.org/10.3763/ijas.2010.0552)  
2 798 2010. 0552
- 3  
4 799 Shiferaw, B., Tesfaye, K., Kassie, M., Abate, T., Prasanna, B.M., Menkir, A., 2014. Managing  
5 800 vulnerability to drought and enhancing livelihood resilience in sub-Saharan Africa:  
6 801 Technological, institutional and policy options. *Weather Clim. Extrem.* 3, 67–79.  
7 802 <https://doi.org/10.1016/j.wace.2014.04.004>
- 8  
9 803 Siatwiinda, S.M., Supit, I., Hove, B. Van, Yerokun, O., 2021. Climate change impacts on rainfed  
10 804 maize yields in Zambia under conventional and optimized crop management.
- 11  
12 805 Steduto, P., Hsiao, T.C., Raes, D., Fereres, E., 2009. AquaCrop—The FAO Crop Model to Simulate  
13 806 Yield Response to Water: I. Concepts and Underlying Principles.  
14 807 <https://doi.org/10.2134/agronj2008.0139s>
- 15  
16 808 Tebaldi, C., Debeire, K., Eyring, V., Fischer, E., Fyfe, J., Friedlingstein, P., Knutti, R., Lowe, J.,  
17 809 O'Neill, B., Sanderson, B., Van Vuuren, D., Riahi, K., Meinshausen, M., Nicholls, Z., Tokarska,  
18 810 K., Hurtt, G., Kriegler, E., Meehl, G., Moss, R., ... Ziehn, T. (2021). Climate model projections  
19 811 from the Scenario Model Intercomparison Project (ScenarioMIP) of CMIP6. *Earth System*  
20 812 *Dynamics*, 12(1), 253–293. <https://doi.org/10.5194/esd-12-253-2021>
- 21  
22 813 Tesfaye, K., Zaidi, P.H., Gbegbelegbe, S., Boeber, C., 2017. Climate change impacts and potential  
23 814 benefits of heat-tolerant maize in South Asia 959–970. [https://doi.org/10.1007/s00704-016-](https://doi.org/10.1007/s00704-016-1931-6)  
24 815 1931-6
- 25  
26 816 Teshome, H., Tesfaye, K., Dechassa, N., Tana, T., Huber, M., 2024. Modeling the Impact of Climate  
27 817 Change on Maize ( *Zea mays* L .) Production and Choice of Adaptation Practices in Eastern  
28 818 Ethiopia. *Int. J. Environ. Res.* <https://doi.org/10.1007/s41742-024-00614-5>
- 29  
30 819 Tian, J., Zhang, Y., Guo, J., Zhang, X., Ma, N., Wei, H., & Tang, Z. (2022). Predicting root zone soil  
31 820 moisture using observations at 2121 sites across China. *Science of the Total Environment*,  
32 821 847(June), 157425. <https://doi.org/10.1016/j.scitotenv.2022.157425>
- 33  
34 822 Trambauer, P., Maskey, S., Winsemius, H., Werner, M., Uhlenbrook, S., 2013. A review of  
35 823 continental scale hydrological models and their suitability for drought forecasting in ( sub-  
36 824 Saharan ) Africa. *Phys. Chem. Earth* 66, 16–26. <https://doi.org/10.1016/j.pce.2013.07.003>
- 37  
38 825 Ullah, I., Shah, S. T., Basit, A., Sajid, M., Arif, M., Ahmad, N., & Noor, F. (2022). Mulching: A New  
39 826 Concept for Climate Smart Agriculture. In K. Akhtar, M. Arif, M. Riaz, & H. Wang (Eds.),  
40 827 *Mulching in Agroecosystems: Plants, Soil & Environment* (pp. 289–313). Springer Nature  
41 828 Singapore. [https://doi.org/10.1007/978-981-19-6410-7\\_17](https://doi.org/10.1007/978-981-19-6410-7_17)
- 42  
43 829 Ullah, H., Santiago-Arenas, R., Ferdous, Z., Attia, A., Datta, A., 2019. Improving water use  
44 830 efficiency, nitrogen use efficiency, and radiation use efficiency in field crops under drought  
45 831 stress: A review. *Adv. Agron.* 156, 109–157. <https://doi.org/10.1016/bs.agron.2019.02.002>
- 46  
47 832 Wang, B., Niu, J., Berndtsson, R., Zhang, L., Chen, X., Li, X., & Zhu, Z. (2021). Efficient organic  
48 833 mulch thickness for soil and water conservation in urban areas. *Scientific Reports*, 11(1), 1–12.  
49 834 <https://doi.org/10.1038/s41598-021-85343-x>
- 50  
51 835 Wang, J. Y., Mo, F., Zhou, H., Kavagi, L., Nguluu, S. N., & Xiong, Y. C. (2021). Ridge–furrow with  
52 836 grass straw mulching farming system to boost rainfed wheat productivity and water use  
53 837 efficiency in semiarid Kenya. *Journal of the Science of Food and Agriculture*, 101(7), 3030–  
54 838 3040. <https://doi.org/10.1002/jsfa.10937>
- 55  
56 839 Wang, P., Deng, Y., Li, X. Y., Wei, Z., Hu, X., Tian, F., Wu, X., Huang, Y., Ma, Y. J., Zhang, C.,  
57 840 Wang, Y., Li, E., & Wang, J. (2019). Dynamical effects of plastic mulch on evapotranspiration  
58 841 partitioning in a mulched agriculture ecosystem: Measurement with numerical modeling.  
59 842 *Agricultural and Forest Meteorology*, 268(September 2018), 98–108.
- 60  
61  
62  
63  
64  
65

843 <https://doi.org/10.1016/j.agrformet.2019.01.014>

1 844 Wang, X., Jia, Z., & Liang, L. (2014). Effect of straw incorporation on soil moisture,  
2 845 evapotranspiration, and rainfall-use efficiency of maize under dryland farming. *Journal of Soil*  
3 846 *and Water Conservation*, 69(5), 449–455. <https://doi.org/10.2489/jswc.69.5.449>

5 847 Zhao, F., Wu, Y., Ma, S., Lei, X., & Liao, W. (2022). Increased Water Use Efficiency in China and  
6 848 Its Drivers During 2000–2016. *Ecosystems*, 25(7), 1476–1492. [https://doi.org/10.1007/s10021-](https://doi.org/10.1007/s10021-021-00727-4)  
7 849 [021-00727-4](https://doi.org/10.1007/s10021-021-00727-4)

9 850 Zhao, H., Qin, J., Gao, T., Zhang, M., Sun, H., Zhu, S., Xu, C., & Ning, T. (2022). Immediate and  
10 851 long-term effects of tillage practices with crop residue on soil water and organic carbon storage  
11 852 changes under a wheat-maize cropping system. *Soil and Tillage Research*, 218(January 2021),  
12 853 105309. <https://doi.org/10.1016/j.still.2021.105309>

14 854 Zhang, X., Kamran, M., Li, F., Xue, X., Jia, Z., Han, Q., 2020. Optimizing fertilization under ridge-  
15 855 furrow rainfall harvesting system to improve foxtail millet yield and water use in a semiarid  
16 856 region, China. *Agric. Water Manag.* 227, 105852. <https://doi.org/10.1016/j.agwat.2019.105852>

18 857 Zhang, P., Wei, T., Han, Q., Ren, X., & Jia, Z. (2020). Effects of different film mulching methods on  
19 858 soil water productivity and maize yield in a semiarid area of China. *Agricultural Water*  
20 859 *Management*, 241(July), 106382. <https://doi.org/10.1016/j.agwat.2020.106382>

22 860 Zhang, Q., Wang, Z., Miao, F., & Wang, G. (2017). Dryland maize yield and water-use efficiency  
23 861 responses to mulching and tillage practices. In *Agronomy Journal* (Vol. 109, Issue 4, pp. 1196–  
24 862 1209). <https://doi.org/10.2134/agronj2016.10.0593>

26 863 Zhao, C., Liu, B., Piao, S., Wang, X., Lobell, D.B., Huang, Y., Huang, M., Yao, Y., Bassu, S., Ciais,  
27 864 P., Durand, J.L., Elliott, J., Ewert, F., Janssens, I.A., Li, T., Lin, E., Liu, Q., Martre, P., Müller,  
28 865 C., Peng, S., Peñuelas, J., Ruane, A.C., Wallach, D., Wang, T., Wu, D., Liu, Z., Zhu, Y., Zhu,  
29 866 Z., Asseng, S., 2017. Temperature increase reduces global yields of major crops in four  
30 867 independent estimates. *Proc. Natl. Acad. Sci. U. S. A.* 114, 9326–9331.  
31 868 <https://doi.org/10.1073/pnas.1701762114>

33 869 Zhang, S., Sadras, V., Chen, X., Zhang, F., 2014. Water use efficiency of dryland maize in the Loess  
34 870 Plateau of China in response to crop management. *F. Crop. Res.* 163, 55–63.  
35 871 <https://doi.org/10.1016/j.fcr.2014.04.003>

37 872 Zizinga, A., Gilbert, J., Mwanjalolo, M., Tietjen, B., Alves, M., Bobe, M., 2024. Maize yield under a  
38 873 changing climate in Uganda : long - term impacts for climate smart agriculture.

40 874 Zizinga, A., Kangalawe, Y.M., Ainslie, A., Tenywa, M.M., Saronga, N.J., Amoako, E.E., 2017.  
41 875 Analysis of Farmer ’ s Choices for Climate Change Adaptation Practices in South-Western  
42 876 Uganda , 1980 – 2009 1–15.

44 877 Zizinga, A., Mwanjalolo, J.-G.M., Tietjen, B., Bedadi, B., Gabiri, G., Luswata, K.C., 2022. Impacts of  
45 878 Climate Smart Agriculture Practices on Soil Water Conservation and Maize Productivity in  
46 879 Rainfed Cropping Systems of Uganda. *Front. Sustain. Food Syst.* 6, 1–12.  
47 880 <https://doi.org/10.3389/fsufs.2022.889830>

49 881

50 882

51  
52  
53  
54  
55  
56  
57  
58  
59  
60  
61  
62  
63  
64  
65